NPS ARCHIVE
1949
IRGENS, D.

Thesis
I57

DUDLEY KNOX LIBRARY
NAVAL POSTGRADUATE SCHOOL
MONTEREY CA 93943-5101

Library
U. S. Naval Postgraduate School
Annapolis, Md.

Minneapolis, Minnesota
July 15, 1949

Faculty Committee
Department of Aeronautical Engineering
University of Minnesota
Minneapolis, Minnesota

Sirs:

Enclosed herewith is completed thesis submitted to you for approval.

Subject thesis is for partial fulfillment of the requirements for a degree of Master of Science in Aeronautical Engineering.

# ANALYSIS OF A
# DOUBLE SKIN AND CORRUGATED
# THIN FLAT PLATE

by

Donald Leroy Irgens

July 15, 1949

IPS ARCHIVE
949
RGENS, D.

# TABLE OF CONTENTS

Summary ---------------------------------Pages 1-2
Introduction ---------------------------- " 3
Equipment and Procedure -------------- " 4-8
Results and Discussion --------------- " 9-12
Conclusions ---------------------------- " 13-14
Sample Calculations ------------------ " 16-17
Appendix A ------------------------------ " 18-25
Bibliography ---------------------------- " 15
Diagrams, Tables and Graphs ----------- " 26-50

# SUMMARY

An experimental investigation was made on the behavior of a test panel constructed of 0.025 aluminum corrugation with 0.032 aluminum skin on both sides. Such a panel was subjected to a compressive load in the longitudinal direction with the unloaded edges simply supported. The panel was long in reference to its width.

Tests showed that inter-rivet buckling induced by inferior blind riveting or too large a rivet spacing would precipitate early panel failure before actual critical load would occur, on a well designed panel.

Such type of construction proved very stable up to loads approaching the critical value. The strength weight ratio indicated it to be very desirable in aircraft construction.

An analytical analysis was made using both non-isotropic and isotropic plate theory; both methods predicted the critical load to within 7.5 per cent of each other, thus indicating that the double skin and corrugation type plate, of the design under consideration, acts much like an isotropic plate.

Because of the fact that such a plate will buckle at a load that will induce strains in the sheet and corrugation above their elastic limits, it was necessary,

in the analytical analysis, to use reduced values for the modulus of elasticity. The prediction of the behavior of the metal in the plastic range is not exact thus indicating such a prediction as critical load is difficult for this type construction.

# INTRODUCTION

The problem under consideration in this report was to study the behavior of a plate of the double skin corrugation construction when subjected to a compression load. Special emphasis was given to the determination of the critical buckling load.

A considerable amount of research work on this type of construction has been carried out by the Glenn L. Martin Aircraft Factory, but considering the complexities that arise in the analysis of any non-isotropic plate, additional research work on it seemed warranted.

The analysis was limited to aluminum alloy plates so designed that the initial buckling stress of the skin and the crippling stress of the corrugation were approximately equal so as to eliminate skin buckling before panel failure.

The experimental tests were limited to a plate loaded with a uniform axial load parallel to the sides of the plate; the unloaded edges were simply supported.

The thesis work was done by the writer during the school year 1948-49 at the University of Minnesota. Thesis advisor was Professor Joseph A. Wise.

# EQUIPMENT AND PROCEDURE

## Test Specimen.

The details of the test panel are shown on Fig. 2.

The material for the panel was furnished by the Glenn L. Martin Aircraft Factory, fabrication of the plate was by the writer.

As noted in Fig. 2 the panel is tapered in planform and thickness, the original plans for the investigation called for a non-tapered section but due to non-availability of desired material the plate was constructed as shown. It was felt that the small amount of taper did not materially change the conditions that would be found in a non-tapered section. For conservatism the minimum section was used for the analytical analysis.

Internal strain gauges with necessary leads were placed before fabrication of cover skins. All strain gauges were placed in duplicate at locations as shown on Fig. 2.

Filler blocks along supported sides so designed to separate skins along supports proved very successful in providing a symmetric support.

Filler blocks at top and bottom of plate designed primarily to transmit the load to the corrugation, were found unnecessary and were removed after initial test.

## Principal Apparatus.

The principal apparatus required for the tests was a suitable jig to support the panel simply along the two unloaded edges; a further non-functional requirement was to make the jig simple and light enough for one man to handle. Such a jig was designed, details of which are shown on Fig. 4.

A 400,000 pound capacity Tinus Olsen testing machine was used for subject tests. The width of the swivel head of the machine corresponded to the width of the top of the panel.

## Minor Apparatus.

The leads from the strain gauges were soldered into a junction box made up with Mallory infant jacks; connections from junction box to Baldwin and Southwark "K" box was by electrical phone plugs.

## Procedure.

The general procedure of the tests was to load the plate by increments, then take strain and deflection readings. It was found that for the load that was placed on the plate during the tests no appreciable deflection was observed, an indication that such type construction is very stable up to critical load.

Three separate tests were made, results of which are shown graphically in Figs. 6 to 14 and in tabular form on Tables I to III.

Tests are described separately below giving details of each.

### Test I.

Load increments of 6,000 pounds were applied; at panel load of 23,000 pounds local failure occurred at top of panel. Upon investigation of local failure it was found that edge supports did not run up high enough, giving an unsupported section of 2 inches at top of plate. Corrective measure taken was to remove the upper 1½ inches of plate, giving only a ½ inch unsupported plate for test number two.

### Test II.

Load increments of 6,000 pounds were applied with one intermediate panel load of 19,850 pounds. Panel load went up to 30,000 pounds at which point local failure occurred at bottom of panel. Upon investigation of local failure it was found that the filler block on bottom did not transmit the load properly to the corrugation and caused a local failure in bearing of the corrugation. This was corrected by trimming 2½ inches from the bottom and removing filler block.

### Test III.

Load increments of 12,000 pounds were applied up to 24,000 pounds, plate remained stable up to 30,000

pounds at which point readings were recorded. Upon increasing the load to 31,600 pounds a failure occurred at approximately 12 inches from the top of the panel. The failure at first appeared to be the critical load for the panel but upon examination of failure it was observed that at point of failure, on one of the cover sheets, one horizontal row of rivets had pulled out thus subjecting the skin to twice its original unsupported length, this reduced the critical buckling stress of the sheet to a point which precipitated the failure.

Above plate load of 30,000 pounds it was observed that inter-rivet buckling had started.

Upon reaching the load where one row of rivets pulled out it appeared as though plate had started to form 3 definite half waves of approximately equal length, the loading was not continued however since another test was to be run on the undamaged remainder.

## Test IV.

Plate was trimmed to a 56 inch length. Load increments were applied similar to those in test three.

Inter-rivet buckling was observed to start at panel load of 31,000 pounds. One definite half wave formed in the longitudinal direction at a load of 34,000 pounds at which point severe inter-rivet buckling occurred on one plate, while other plate remained flat. Maximum deflection of half wave was at center of plate and was estimated

to be one and one half inches, since deflection was greater than Ames dial capacity at that point.

## RESULTS AND DISCUSSION

Load, strain data is presented on Tables I-IV. The principal strains were obtained from rosette readings by method described in Reference 2 of bibliography. Plots of principal stresses versus plate loads are shown on Figs. 5-14.

It was unfortunate that none of the four tests produced a true critical load on the plate, however, it was felt that the tests proved successful as they clearly showed the stability of this type construction in the region of design load. The indications of the tests were such that the panel would be well in its plastic range before the critical load would be reached; a theoretical analysis, which will be presented subsequently, bears this fact out quite clearly.

Inasmuch as the critical load on a panel such as this is of no practical value, it is used extensively as a design criteria, that is by being able to predict what the critical load is and knowing the behavior of the plate up to critical, a safe design load may be arrived at.

The tests bore out the fact that any rivet failure will induce early skin instability, it appeared that had the rivet spacing been decreased to three fourths of an inch, the skin would have remained stable and

probably would have allowed the plate to reach a full critical value.

## Theoretical Analysis.

The method used in the theoretical analysis follows quite closely the work as presented in Reference 1.

The critical load on a non-isotropic plate similarly loaded and supported to the one of this test is given in Reference 3 as:

$$P_{CR} = \frac{2\pi^2}{b^2} \sqrt{(D_x)(D_y)} + D_3$$

where: $P_{CR}$ = critical load in pounds per unit width

$b$ = plate width, small in reference to length

$D_x$ = average flexural rigidity per unit width of the plate parallel to the y axis

$D_y$ = same as $D_x$ but parallel to x axis

$D_3 = \frac{1}{2}\left[\mu D_y + \mu D_x\right] + 2(GI)_{xy}$

$2(GI)_{xy}$ = average torsional rigidity of the plate (ratio of the moment per unit width to the twist)

also: $D_x = \dfrac{(EI)_x}{1 - \mu_x\mu_y}$ , $D_y = \dfrac{(EI)_y}{1 - \mu_x\mu_y}$

Since flexural rigidity about an axis parallel to y is contributed to by both sheet and corrugation, and about an axis parallel to x is contributed mainly by sheet, $D_x$ and $D_y$ are conservatively written as:

$$D_x = \frac{(E_{sheet} I_{sheet})_x}{1 - \mu^2} + (E_{corr} I_{corr})_x$$

$$D_y = \frac{(E_s I_s)_x}{1 - \mu^2}$$

For further conservatism effect of corrugation in $D_x$ is omitted in evaluation of $D_3$, hence:

$$D_3 = \frac{(E_s I_s)_x}{1 - \mu^2} + 2(GI)_{xy}$$

In Reference 1 it is shown that the term $2(GI)_{xy}$ is a constant and can be replaced by $G_e t_s d^2$, where:

$G_e$ = effective shear modulus

$t_s$ = bare skin thickness

d = distance between skins

Tests conducted on corrugation columns at the Glenn L. Martin Company indicate that the tangent modulus of elasticity of the compression stress strain curve can be used to predict the value of $E_c$ for the type plate in question, hence Fig. 18 was plotted from properties as given in Fig. 17.

$(E_s)_x$ is also taken as the tangent modulus of the average strain strain curve from the properties of flat sheet when the critical buckling load has been exceeded. Such a curve is plotted on Fig. 20 from data of Fig. 19. For conservatism $(E_s)_y$ has been taken as equal to $(E_s)_x$.

Effective shear modulus has been studied quite extensively for this type construction in Reference 1,

and a value of 0.7 G has proved to be quite reliable for cases of the plate being stressed above the elastic limit.

By assuming a series of maximum strains and calculating $P_{CR}$ by the non-isotropic plate equation just given, then finding corresponding load a stable plate will carry at similar strains by $P'_{CR} = \sigma_{corr} A_{corr} + \sigma_{sheet} A_{sheet}$ and plotting results, the intersection of two plots will give predicted critical load for panel; such a plot is given on Fig. 21. A typical calculation for making the graph is given under Sample Calculations of this thesis.

The predicted critical load was determined to be 2,900 pounds per inch of width; for an average width of 17 inches between supports this would correspond to a total panel load of 49,300 pounds. Maximum strain in plate at critical load was predicted at 0.00345 inches per inch.

This theoretical analysis indicates the plate goes well into the plastic range of the material before critical load is obtained. In reference to actual test results it can be readily seen that plate was obeying Hooke's Law almost up to the point where local skin buckling precipitated panel failure, and that if skin had not buckled prematurally load could have continued up to near predicted critical.

# CONCLUSIONS

Corrugation and double skin type of construction forms a very stable panel and maintains this stability very close to its critical load. The strength weight ratio is very high, a factor of significance in aircraft construction.

Relating the test results to theoretical calculations indicates that a design load critical load ratio is in the neighborhood of 0.6.

The need for precise riveting and rigid inspection after completing a panel seems very necessary since panels of this type depend largely on the flexural rigidity contributed by the sheets, for stability.

The test results did not indicate a true critical load, however had inter-rivet buckling been suppressed by a more precise rivet job or a decreased rivet spacing it is believed the actual and predicted critical load would have approached each other.

The analytical analysis is by no means an exact one, since various assumptions as to the behavior of the plate in the plastic range have been made, however it appears quite reliable in reference to repeated applications by the Glenn L. Martin Aircraft Company.

The plate apparently can be treated as an isotropic plate based on the analysis of an isotropic plate by

the method of strain energy, as given in Appendix A. The analysis as given in Appendix A predicts a critical load about 7.5 per cent higher than by analyzing the plate as being non-isotropic.

# BIBLIOGRAPHY

1. Kennedy, W. B., Troxell, W. W.: Study of Compression Panel Supported on Four Edges, Formed of Corrugated Sheet with Flat Skin on Both Sides. Structural Development Report 21, Glenn L. Martin Company, 1944.

2. Wise, Joseph A.: Circles of Strain. Journal of the Aeronautical Sciences, Vol. 7, No. 10, pp. 438-40, August 1940.

3. Timoshenko, S.: Theory of Elastic Stability, McGraw-Hill Book Company, 1936.

# SAMPLE CALCULATIONS

For: $P_{cr} = \frac{2\pi^2}{b^2}\left[\sqrt{(D_x)(D_y)} + D_3\right]$ Ref. page Fig. 21

$P'_{cr} = \sigma_{corr.} A_{corr} + \sigma_{sheet(Ave.)} A_{sheet}$

[illegible]: $\epsilon_{n}$ = 0.0038 in/in

Constants. $G_c = \frac{E}{2(1+\mu)}$ = [illegible] E

$E = 10^7$ below [illegible] limit

$I_s = 0.005475$ in.$^4$/in, $A_s$ = [illegible] in$^2$/in

$I_c = 0.00159$ in.$^4$/in, $A_c = 0.0375$ in$^2$/in

d = [illegible] in. min, distance between skins

$t_s$ = 0.0272 in. {bare 0.032 Alclad}

$t_c$ = 0.022 in {bare 0.025 Alclad}

b = 15.0 in. {average width of plate}

$\mu$ = 0.3 $(1-\mu^2)$ = 0.91

$\frac{2\pi^2}{b^2} = 0.08716$, $E_c$ see Fig. 20, $E_s$ see Fig. 18

$G t_s d^2$ = 49,[illegible], $\sigma_{corr}$ see Fig. 19, $\sigma_{sheet}$ see Fig. 19

$\therefore$ $D_x = \frac{1.6\times10^6 \times .005475}{0.91} + 7.4\times10^6(.00159)$

$= 9625 + 11,750 = 21,375$ lb in.

$D_y$ = 9625 lb in., $D_3$ = [illegible](9625) + 0.71([illegible]) = 31,445

$P_{cr} = .08716\left[10^3\sqrt{(.021375)(.009625)} + 31,445\right]$

$P_{cr}$ = [illegible] lbs/in.

[illegible]

$P'_{cr}$ = (38,[illegible])(.0375) + ([illegible])(.024) = 3138 lbs/in

## SAMPLE CALCULATIONS (Con't)

Reduction of 45° strain rosette data to principal strains. (Ref. 2)

Test #1 Load = 13,415# Table #I

Sheet #1 45° Rosette 38 in from top.

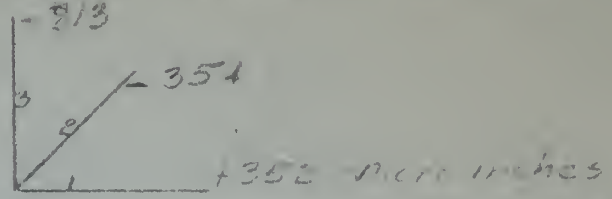

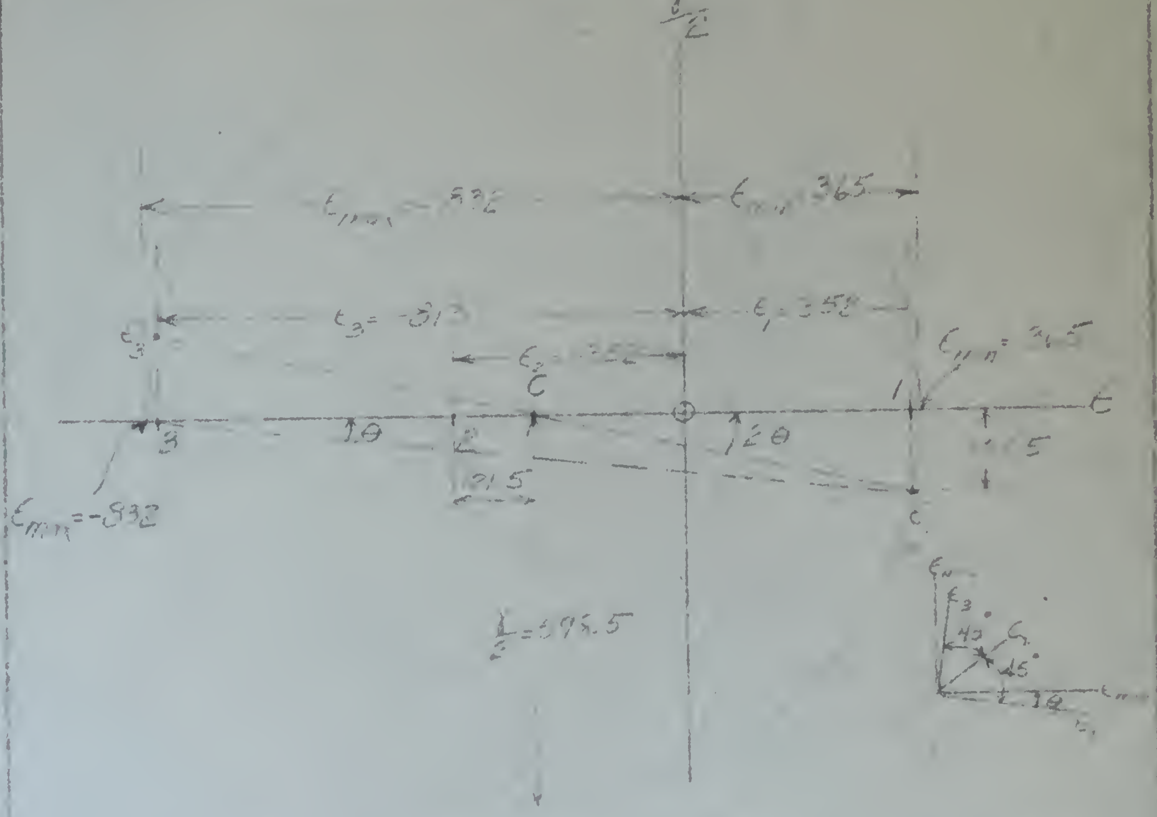

C is mid point between 1 and 3
[illegible]

$$\sigma_{max} = \frac{E}{1-\mu^2}\left[\epsilon_{max} + \mu\epsilon_{min}\right], \quad \sigma_{min} = \frac{E}{1-\mu^2}\left[\epsilon_{min} + \mu\epsilon_{max}\right]$$

# Appendix A

[illegible] of [illegible] applied
to the isotropic plate theory.

Theoretical analysis by method of strain energy.
General expression for internal strain energy.

$U_i = \int \frac{1}{2}\sigma\epsilon\, dV$

By assuming a configuration for a deflection curve, an expression expressing the internal and external strain energy can be worked out.

∴ Assume loading, deflection and configuration of isotropic plate to be as shown below:

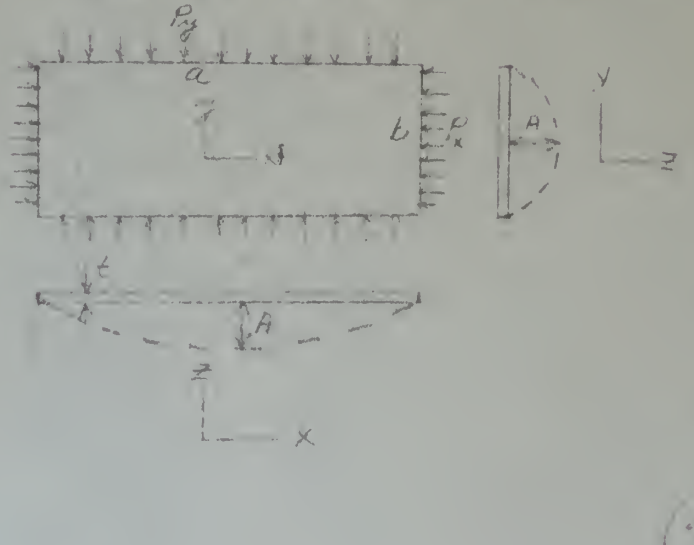

Assume a shape

$z = A\sin\frac{m\pi x}{a}\sin\frac{n\pi y}{b}$

Where: A, max. defl.
m = Number of half sin waves in x dir.
n = Number of half sin waves in y dir.
(sketch shows m=n=1)

By expressing stresses and strains in terms of deflection curve as shown.

$\sigma_x = \frac{E}{1-\mu^2}\, z\left[\frac{\partial^2 z}{\partial x^2} + \mu\frac{\partial^2 z}{\partial y^2}\right]$

$\epsilon_x = z\frac{\partial^2 z}{\partial x^2}$

$$\sigma_y = \frac{E}{1-\mu^2}\, z\left[\frac{\partial^2 w}{\partial y^2} + \mu\frac{\partial^2 w}{\partial x^2}\right]$$

$$\epsilon_y = z\,\frac{\partial^2 w}{\partial y^2}$$

$$\tau'_{xy} = G\gamma'_{xy} = \frac{E}{2(1+\mu)}\,2z\,\frac{\partial^2 w}{\partial x\,\partial y}$$

$$\gamma'_{xy} = 2z\,\frac{\partial^2 w}{\partial x\,\partial y}$$

Expression for internal strain energy becomes:

$$U_i = \frac{1}{2}\int_{-\frac{t}{2}}^{\frac{t}{2}}\left[\frac{Ez^2}{1-\mu^2}\left\{\left(\frac{\partial^2 w}{\partial x^2} + \mu\frac{\partial^2 w}{\partial y^2}\right)\frac{\partial^2 w}{\partial x^2} + \left(\frac{\partial^2 w}{\partial y^2} + \mu\frac{\partial^2 w}{\partial x^2}\right)\frac{\partial^2 w}{\partial y^2}\right\} + \frac{2E\cancel{z^2}}{2(1+\mu)}\left(\frac{\partial^2 w}{\partial x\,\partial y}\right)^2\right]dz$$

Since $\int_{-\frac{t}{2}}^{\frac{t}{2}} z^2\,dz$ is [illegible] equal to $I$ expression reduces to:

$$U_i = \frac{EI}{2(1-\mu^2)}\iint\left[\left(\frac{\partial^2 w}{\partial x^2}\right)^2 + \left(\frac{\partial^2 w}{\partial y^2}\right)^2 + 2\mu\frac{\partial^2 w}{\partial x^2}\frac{\partial^2 w}{\partial y^2} + 2(1-\mu)\left(\frac{\partial^2 w}{\partial x\,\partial y}\right)^2\right]dx\,dy$$

For expression for external strain energy

$U_e = \frac{1}{2}\int \sigma\,dA$ where $dA$ is [illegible] [illegible] [illegible]

$\therefore\ 0 = L_{max} - L_{min}$ [illegible]

$\therefore\ L_{min}$ [illegible]

By expansion in binomial theorem

$$L_c = \int_0^l \left[1 + \frac{1}{2}\left(\frac{\partial w}{\partial y}\right)^2 + \dots\right] dy$$

$$\therefore \Delta l = L_c - L_{c_0} = \frac{1}{2}\left(\frac{\partial w}{\partial y}\right)^2$$

$$\therefore \underline{V_e = \frac{1}{2}\int P\left(\frac{\partial w}{\partial y}\right)^2 dy}$$

For given case

$$\int\left(\frac{\partial^2 w}{\partial x^2}\right)^2 dA = \frac{m^4\pi^4 f^2 b}{4a^3}$$

$$\int\left(\frac{\partial^2 w}{\partial y^2}\right)^2 dA = \frac{n^4\pi^4 f^2 a}{4b^3}$$

$$\int\left(\frac{\partial^2 w}{\partial x^2}\cdot\frac{\partial^2 w}{\partial y^2}\right) dA = \frac{m^2 n^2\pi^4 f^2}{4ab}$$

$$\int\left(\frac{\partial^2 w}{\partial x \partial y}\right)^2 dA = \frac{m^2 n^2\pi^4 f^2}{4ab}$$

$$\therefore V_i = \frac{EI}{2(1-\mu^2)}\left[\frac{\pi^4 f^2}{4a^3b^3}\right]\left[m^4b^4 + n^4a^4 + 2\mu(m^2n^2a^2b^2) + 2(1-\mu)(m^2n^2a^2b^2)\right]$$

or

$$V_i = \frac{EI}{2(1-\mu^2)}\frac{\pi^4 f^2}{4a^3b^3}\left[\left(m^2b^2 + n^2a^2\right)^2\right]$$

and

$$V_e = \iint \frac{P}{2}\,\frac{m^2\pi^2 f^2}{a^2}\cos^2\frac{m\pi x}{a}\sin^2\frac{n\pi y}{b}\,dx\,dy + \iint \frac{P}{2}\,\frac{n^2\pi^2 f^2}{b^2}\sin^2\frac{m\pi x}{a}\cos^2\frac{n\pi y}{b} \dots$$

or $V_e = \frac{1}{2} A^2\pi^2 \left[\frac{f_x m^2 b}{4a} + \frac{f_y n^2 a}{4b}\right]$

then equate $V_e = V_a$ for equilibrium of plate, this gives:

$$\left[f_x m^2 b^2 + f_y n^2 a^2\right] = \frac{EI}{(1-\mu^2)} \cdot \frac{\pi^2}{a^2 b^2} \left(m^2 b^2 + n^2 a^2\right)^2$$

For conditions of test $f_y = 0$

Since the double skin and corrugation type plate will not buckle before reaching the elastic limit of the material it is necessary to use a reduced modulus in predicting a critical load. The method used in arriving at effective values of $E$ in the non-isotropic analysis will be used here.

By assuming various combinations of half waves in above developed equation the minimum $f$ loading thus obtained will be the critical loading of the plate. The wave formation in the short dimension for such a case can be proven to be always in a $\frac{1}{2}$ wave.

[illegible]

[illegible]

[illegible]

[illegible]

[illegible] (See Fig. 18)

[illegible] 17)

[illegible] 20

[illegible] 19)

[illegible]

[illegible]

[illegible]

[illegible]

[illegible]

[illegible]

[illegible]

[illegible]

[illegible]

[illegible]

[illegible]

[illegible] [illegible] symmetric [illegible] plate [illegible] takes the form of five or four buckles in the long direction (and [illegible] short direction)

[illegible] from the moduli as was done for isotropic theory to check [illegible] the result theory)

[illegible]

∴ at [illegible] conditions

$P_{cr} = (38,000)(0.375) + (26,300)(.064) = $ [illegible] $lb/in$

For any given plate the procedure would be to assume various maximum strains at which plate would reach critical load in these strains obtain Effective Modulus of Elasticity of corrugation and sheet and corresponding stresses in the materials at assumed strains. Then up results similarly to that of Fig 21 which will produce critical load of plate.

From above isotropic analysis the

Predicted critical load for plate was 3120 lbs/in. whereas non-isotropic plate theory gives a value of 2800 pounds per inch of width.

The difference is relatively small which indicates the plate acts much as an isotropic plate.

The slightly higher value obtained using the isotropic plate theory was mainly due to the fact that the flexural rigidity of the plate was due to both the sheet and corrugation about both the x and y axis, whereas in the non-isotropic theory, the contribution of the corrugation to the flexural rigidity about an axis parallel to the corrugation was omitted.

Fig. 2

Diagram of Test Panel

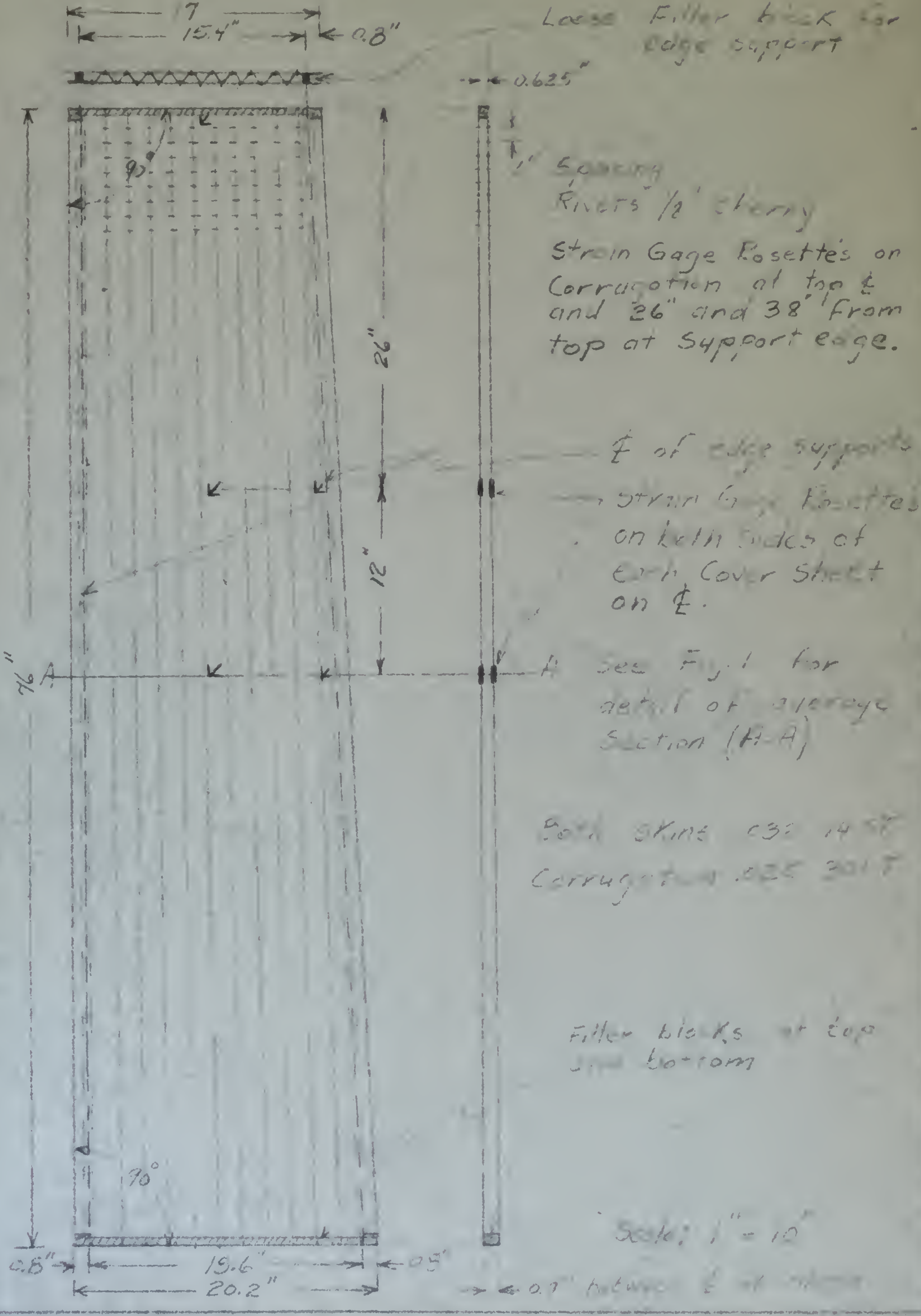
17"
15.4"
0.8"
Loose Filler block for edge support
0.625"
90°
1" Spacing
Rivets 1/8" Cherry
Strain Gage Rosette's on Corrugation at top ℄ and 26" and 38" from top at Support edge.
26"
12"
76"
A
A
℄ of edge supports
Strain Gage Rosettes on both sides of Each Cover Sheet on ℄.
See Fig. 1 for detail of average Section (A-A)
Both skins .032 24 ST
Corrugation .025 24 ST
Filler blocks at top and bottom
90°
Scale; 1" = 10"
0.8"
19.6"
0.5"
20.2"
0.7" between ℄ of skins

Fig. 3

Panel Loading Diagram

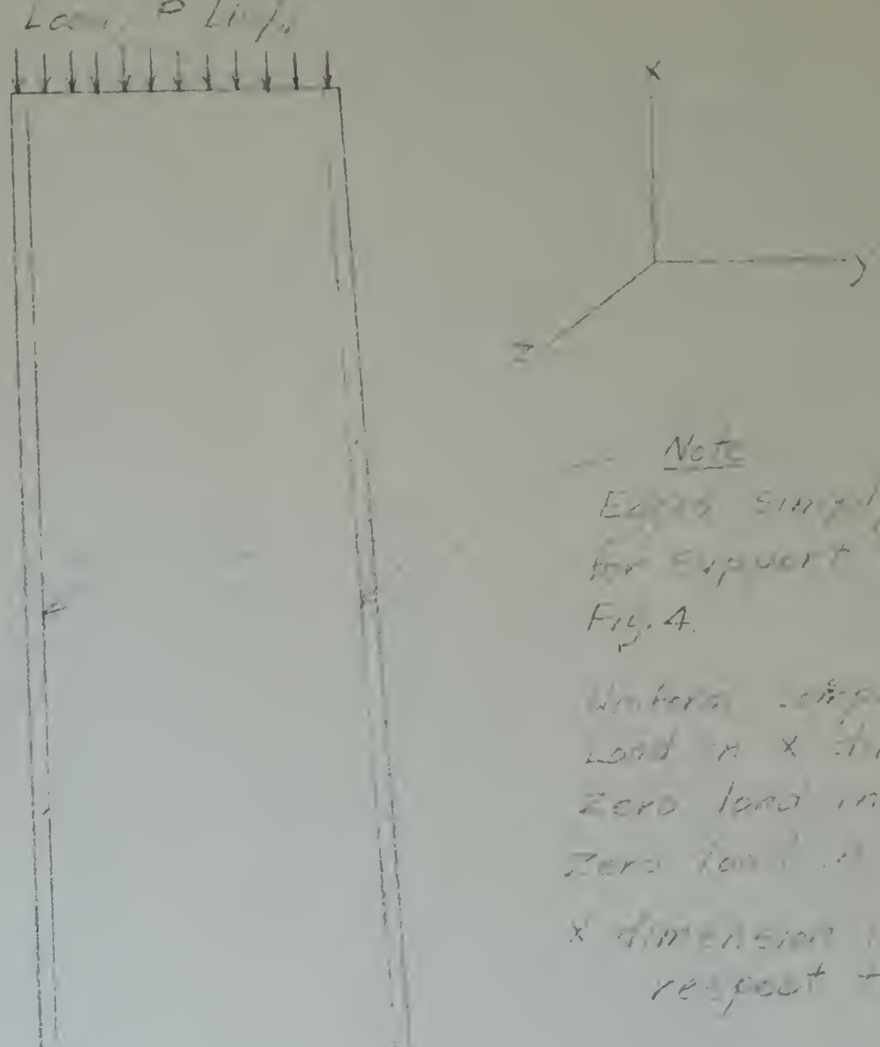

Note

Edges simply supported, for support detail see Fig. 4.

Uniform compression load in x direction.

Zero load in y direction.

Zero load in z direction.

x dimension is large with respect to y.

Fig. 4

Diagram of Testing Jig

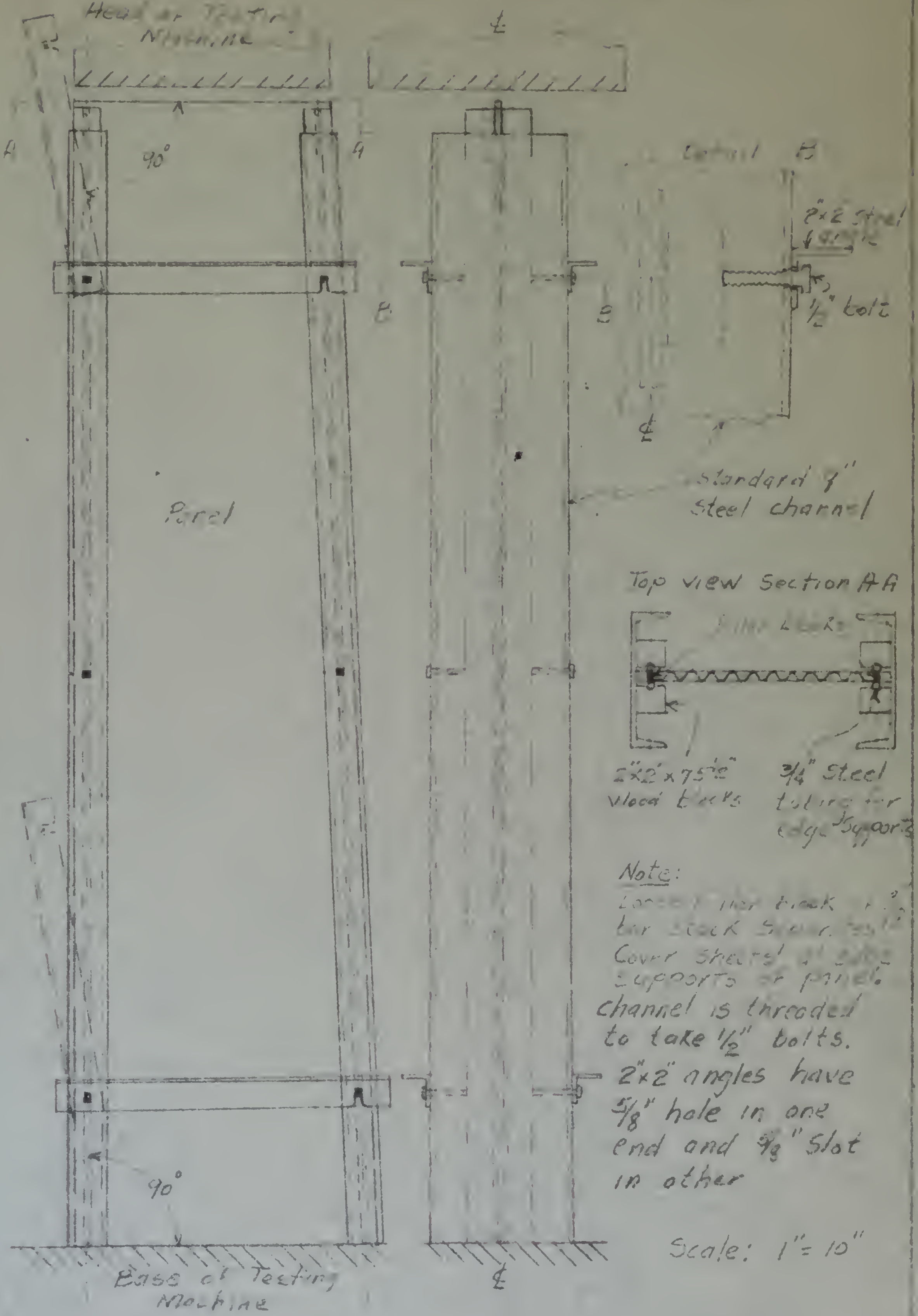

Note:
[illegible] block [illegible] bar stock [illegible] Cover sheets at edge supports of panel.
channel is threaded to take ½" bolts.
2"×2" angles have ⅝" hole in one end and ⅝" slot in other

Scale: 1" = 10"

Table I

Test #1

$\mu = 0.3$, $E = 10^7$

Plotted on Figs 5-6-7

| Gage location | Gage No. | Panel load 6000 lbs. | | | Panel load 12,000 lbs. | | | Panel load 18,000 lbs. | | |
|---|---|---|---|---|---|---|---|---|---|---|
| | | Strain Micro inches | Stress lbs/in² | Shear lbs/in² | Strain | Stress | Shear | Strain | Stress | Shear |
| Plate 1 | | | | | | | | | | |
| 38 in from top on ℄ Vert | 19-25- | -281 | | | -540 | | | -813 | | |
| " Horz | 19-26- | +121 | | | +250 | | | +352 | | |
| " 45° | 21-28- | -132 | | | -225 | | | -354 | | |
| Principal | | -290 | -2760 | | -550 | -5145 | | -832 | -7735 | |
| | | +130 | +473 | 1616 | +260 | +1045 | 3215 | +365 | +1270 | 4603 |
| Plate 2 | | | | | | | | | | |
| 26 in. from top on ℄ Vert | 1-8- | -260 | | | -504 | | | -753 | | |
| " Horz | 2-9 | +79 | | | +132 | | | +204 | | |
| " 45° | 3-10- | -131 | | | -235 | | | -357 | | |
| Principal | | -265 | -2675 | | -506 | -5120 | | -762 | -7670 | |
| | | +85 | +60 | 1347 | +135 | -185 | 2427 | +214 | -161 | 3754 |
| 38" from top on ℄ Vert | 4-11 | -235 | | | -450 | | | -741 | | |
| " Horz | 5-12- | +56 | | | +162 | | | +262 | | |
| " 45° | 7-14- | -135 | | | -240 | | | -340 | | |
| Principal | | -243 | -2465 | | -491 | -4930 | | -750 | -7350 | |
| | | +63 | -110 | 1177 | +172 | +272 | 2551 | +270 | +605 | 3977 |
| Corrugation | | | | | | | | | | |
| 26 in. from top on edge Vert | 37-44- | -96 | | | -360 | | | -574 | | |
| " Horz | 38-45 | +61 | | | +132 | | | +191 | | |
| " 45° | 39-46 | -65 | | | -130 | | | -200 | | |
| Principal | | -100 | -775 | | -362 | -3576 | | -545 | -5350 | |
| | | +75 | +465 | 708 | +134 | +279 | 1907 | +192 | +313 | 2832 |
| 38 in. from top on edge Vert | 40-47 | -208 | | | -466 | | | -611 | | |
| " Horz | 41-48- | +75 | | | +159 | | | +235 | | |
| " 45° | 43-50- | -74 | | | -151 | | | -245 | | |
| Principal | | -211 | -2030 | | -477 | -3950 | | -615 | -5970 | |
| | | +68 | +272 | 1151 | +160 | -717 | 2154 | +240 | +605 | 3287 |

[illegible]

| | | | | | | | | | | | | | | |
|---|---|---|---|---|---|---|---|---|---|---|---|---|---|---|
| Plate 1 | | | | | | | | | | | | | | |
| 3-1 in from top on ℄ Vert 15 22 | -752 | | | -515 | | | -779 | | | -815 | | | -1022 | | |
| " Horiz 19 | +125 | | | +[illegible] | | | +338 | | | -344 | | | +482 | | |
| " 45° 3/1 | 185 | | | -205 | | | -339 | | | -355 | | | -397 | | |
| Principal | -261 | -250 | | [illegible] | -4440 | | -[illegible] | -[illegible] | 1206 | -545 | -[illegible] | | -1039 | -1705 | |
| | +134 | +[illegible] | 1574 | +28 | +137 | 3[illegible] | +[illegible] | +697 | 4678 | +40 | 1186 | 4805 | +775 | +1842 | 5846 |
| Plate 2 | | | | | | | | | | | | | | | |
| 24½ in from top on ℄ Vert | -253 | | | -405 | | | -774 | | | -854 | | | -1079 | | |
| " Hor | +81 | | | +22[illegible] | | | +298 | | | +[illegible] | | | +759 | | |
| " 45° | -70 | | | -168 | | | -250 | | | -280 | | | -345 | | |
| Principal | -255 | -2500 | | -406 | -4675 | | -774 | -1785 | | -855 | -8210 | | -1082 | -10,41[illegible] | |
| | +[illegible] | +605 | [illegible] | +201 | +617 | 2641 | +298 | +158 | 4177 | +361 | +115 | 4650 | +730 | +[illegible] | 5573 |
| 36½ in from top on ℄ Vert | -2[illegible] | | | | | | | | | | | | | | |
| " Horiz | +77 | | | | | | | | | | | | | | |
| " 45° | -5[illegible] | | | | | | | | | | | | | | |
| Principal | -[illegible] | -3[illegible] | | -4[illegible] | [illegible] | | -709 | -[illegible] | | -854 | -[illegible] | | -1046 | -[illegible] | |
| | +[illegible] | +77 | 1536 | +[illegible] | +[illegible] | [illegible] | +[illegible] | +[illegible] | 4[illegible] | +[illegible] | +1256 | 4115 | +[illegible] | +[illegible]41 | 5[illegible] |
| [illegible] from top Vert 37 44 | -166 | | | -357 | | | -546 | | | -660 | | | -[illegible] | | |
| [illegible] | +[illegible] | | | +160 | | | +225 | | | +260 | | | +310 | | |
| " 45° | -4[illegible] | | | -1[illegible] | | | -182 | | | -230 | | | -270 | | |
| Principal | -167 | -[illegible] | | -[illegible] | -[illegible] | | -541 | -5[illegible] | | -661 | -6400 | | -[illegible] | [illegible] | |
| | +130 | +219 | 71[illegible] | +118 | +123 | 1822 | +226 | +[illegible] | 2[illegible] | +161 | +685 | 3541 | +[illegible] | -[illegible] | 4[illegible] |
| [illegible] from top [illegible] edge Vert 17 | -137 | | | -45[illegible] | | | -670 | | | -786 | | | -910 | | |
| Hor 48 | +[illegible] | | | +[illegible] | | | +160 | | | +225 | | | +310 | | |
| 45° 50 | -[illegible] | | | -12[illegible] | | | -200 | | | -235 | | | -280 | | |
| Principal | -[illegible] | -1370 | | -4[illegible] | -4[illegible] | | -[illegible] | -[illegible] | | -788 | 7700 | | -[illegible] | -[illegible] | |
| | +[illegible] | -308 | 543 | +[illegible] | -225 | [illegible] | +164 | -417 | 3121 | +227 | -1035 | 3437 | +[illegible] | +41[illegible] | 4[illegible] |

| [illegible] | [illegible] | [illegible] | [illegible] | Shear | [illegible] | [illegible] | [illegible] | [illegible] | [illegible] | [illegible] |
|---|---|---|---|---|---|---|---|---|---|---|
| Plate 1 | | | | | | | | | | |
| 36½ in from top on ℄ Vert | 19<br>25- | -623 | | | 1278 | | | -1695 | | |
| " Horiz | 2<br>22- | +270 | | | +516 | | | +600 | | |
| " 45° | 21<br>28- | -230 | | | -520 | | | -840 | | |
| Principal | | -632 | -6040 | | -1290 | -12,430 | | -1740 | -17,000 | |
| | | +274 | +927 | 3484 | +523 | +1434 | 6762 | +640 | +1997 | 9148 |
| Plate 2 | | | | | | | | | | |
| 34½ in from top on ℄ Vert | 1<br>8 | -494 | | | -930 | | | -1015 | | |
| " Horiz | 2<br>9- | +202 | | | +410 | | | +540 | | |
| " 45° | 3<br>10- | -175 | | | -350 | | | -330 | | |
| Principal | | -500 | 4820 | | -940 | -8950 | | -1023 | -9430 | |
| | | +205 | +605 | 2762 | +420 | +1517 | 5238 | +550 | +2560 | 5995 |
| 36½' from top on ℄ Vert | 4<br>11- | -475 | | | -985 | | | | | |
| " Horiz | [illegible] | [illegible] | | | +455 | | | | | |
| " 45° | 7<br>14- | -178 | | | -399 | | | | | |
| Principal | | -480 | -4570 | | -1000 | -9575 | 1 | -1180 | -10910 | |
| | | +213 | +751 | 2264 | +461 | +1770 | 5612 | +631 | +3045 | 6978 |
| Corrugation 36½" from top on edge Vert | 40<br>47 | -519 | | | 1040 | | | -1320 | | |
| " Horiz | 41<br>48 | +175 | | | +310 | | | +480 | | |
| " 45° | 43<br>50 | -135 | | | -340 | | | -440 | | |
| Principal | | -522 | -5150 | | -1042 | -10430 | | -1321 | -12,820 | |
| | | +177 | +224 | 2287 | +311 | -44 | 5198 | +481 | +932 | 6376 |

[illegible]

# Table IV

Test # [illegible]     Plates on Fig. 14

| Gage location | Gage No. | First load 12,000 lbs<br>Strain micro in. per in. | Stress lbs/in² | Shear lbs/in² | Second load [illegible] lbs<br>Strain | Stress | Shear | Third load [illegible] lbs<br>Strain | Stress | Shear |
|---|---|---|---|---|---|---|---|---|---|---|
| Plate [illegible] | | | | | | | | | | |
| Web, [illegible] from top on ℄ Vert | 18-25- | -570 | | | -1160 | | | | | |
| " Horiz | 19-2- | +200 | | | +730 | | | | | |
| " 45° | 21-18- | -345 | | | -500 | | | | | |
| Principal | | -57[illegible] | -5[illegible] | | -1170 | | | | | |
| | | +212 | +1581 | 2[illegible]94 | +4[illegible] | | | | | |
| Compression [illegible] | [illegible] | -670 | | | -1190 | | | -4[illegible] | | |
| 12 in. from [illegible] on edge Vert | [illegible] | +195 | | | -345 | | | +553 | | |
| " Horiz | [illegible] | -170 | | | -360 | | | -500 | | |
| " 45° | | -640<br>+1[illegible] | [illegible]<br>[illegible] | [illegible] | -1191<br>+346 | [illegible]<br>-1[illegible] | [illegible] | -5[illegible]<br>+550 | [illegible]<br>+[illegible] | [illegible] |
| Principal | | | | | | | | | | |

Fig. 2

Plate Load vs. Max. Cover Shear(1) Stress

(Test #1, Re. Table I)

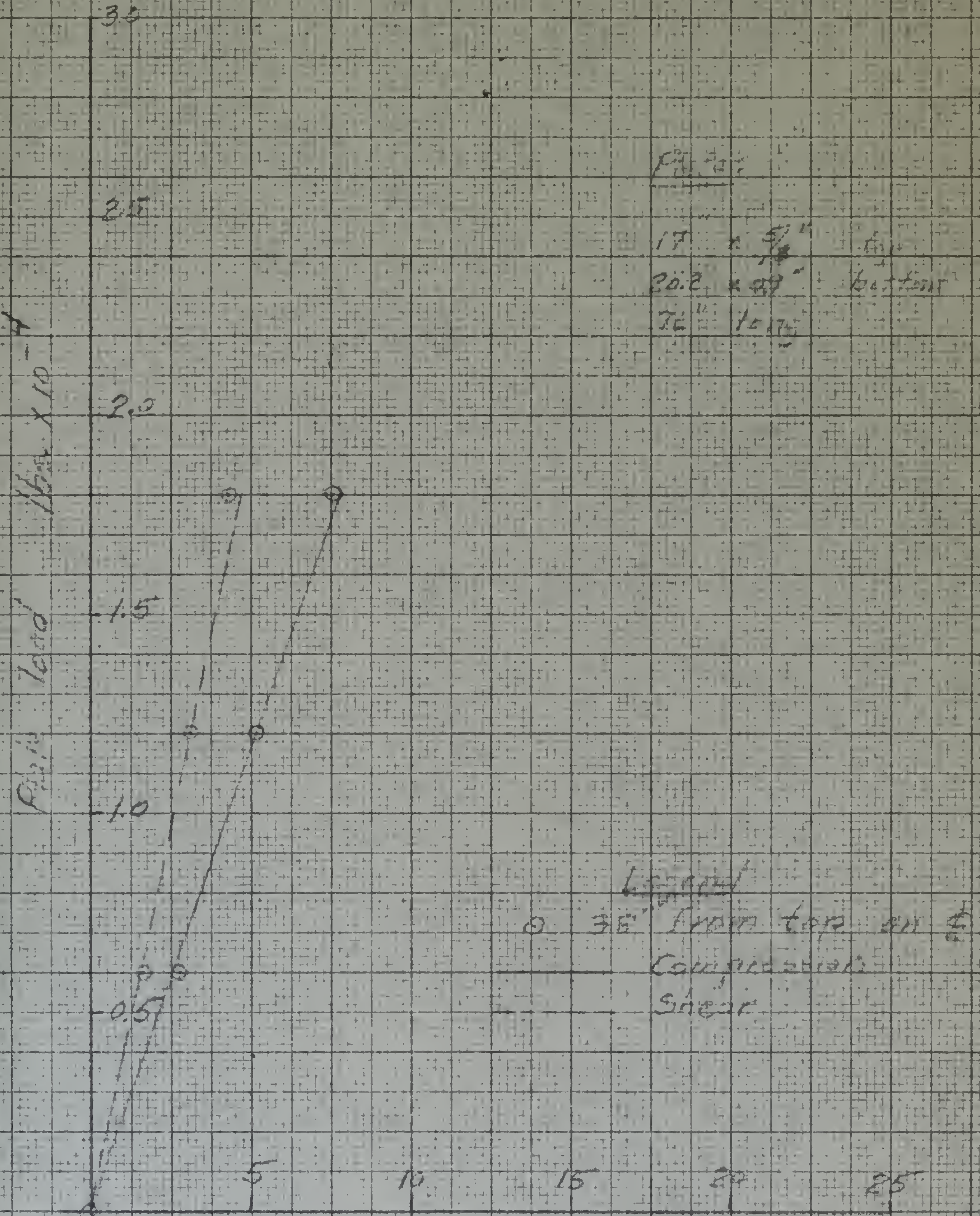

Fig 6

Plate Load vs. Max. Cover Sheet (2) Stress

(Test #1)

Ref Table I

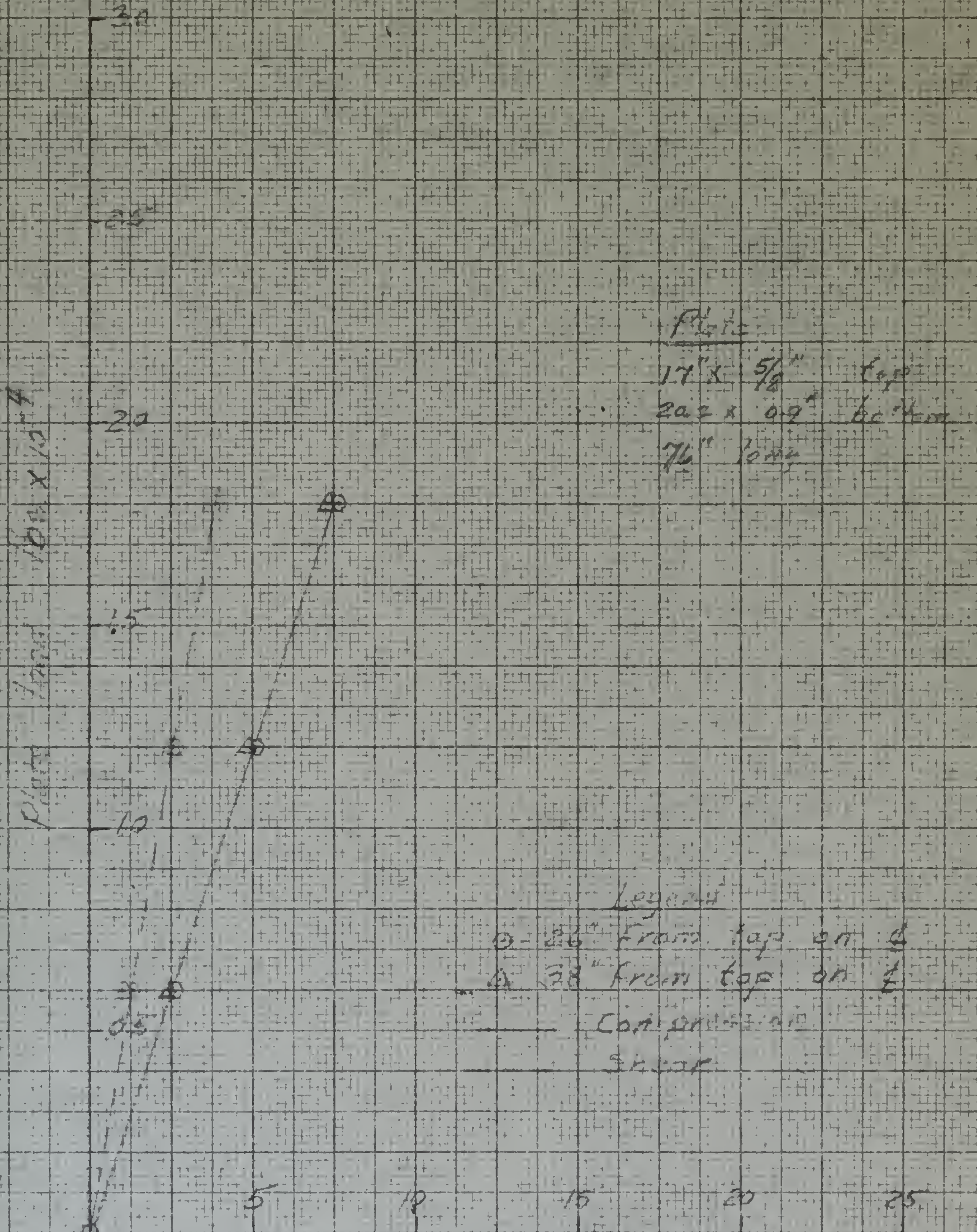

Fig. 7

Plate Load vs. Max Corrugation Stress
(Test #1)
Ref. Table I

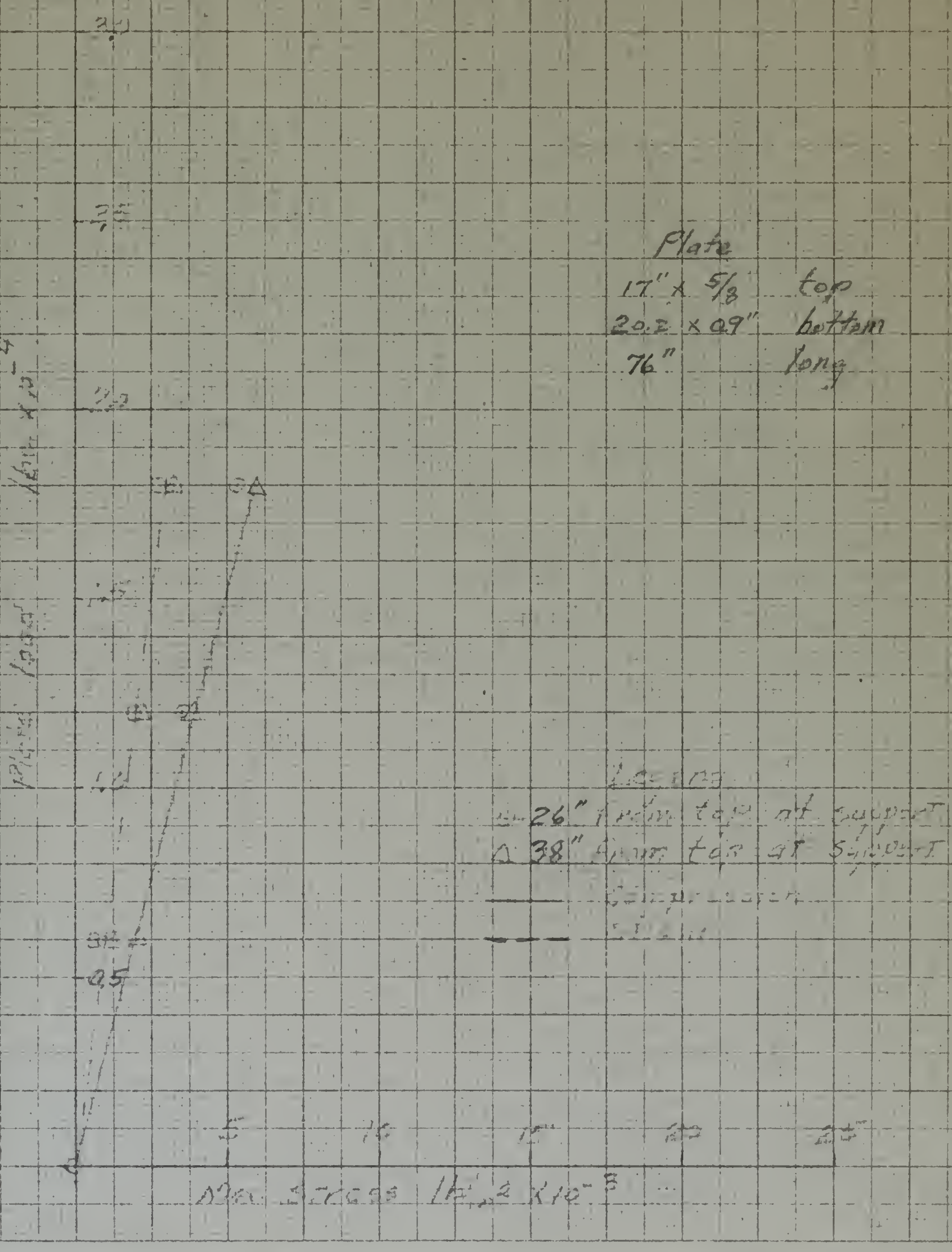

Plate
17" x 5/8 top
20.2 x 0.9" bottom
76" long

Fig. 1

Plate Load vs. Wire Cover sheet(1) Stress
(Test #2)

Ref Table II

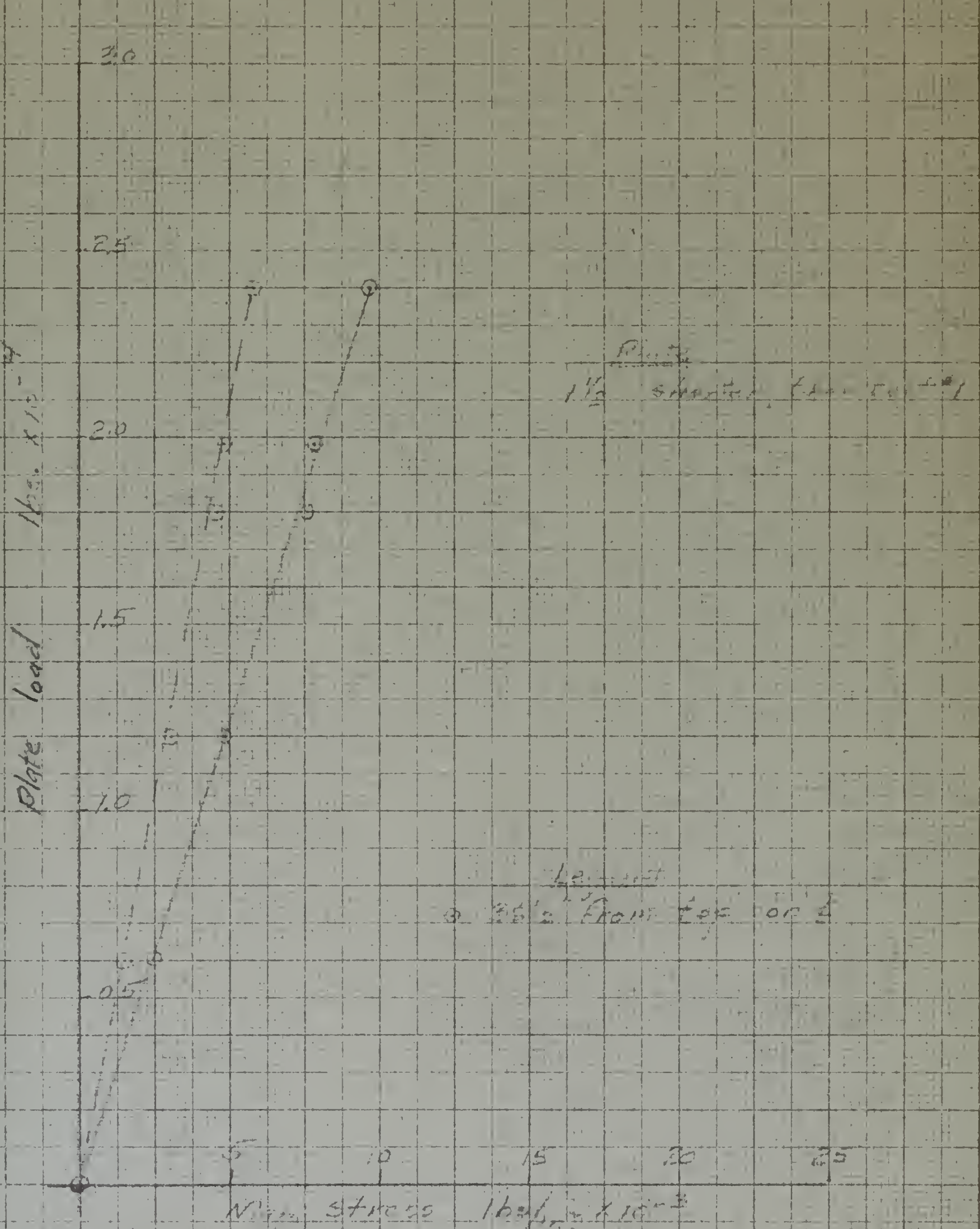

Fig 2

Plate Load vs. Max. Compressive Stress
(Test #2)
Ref Table II

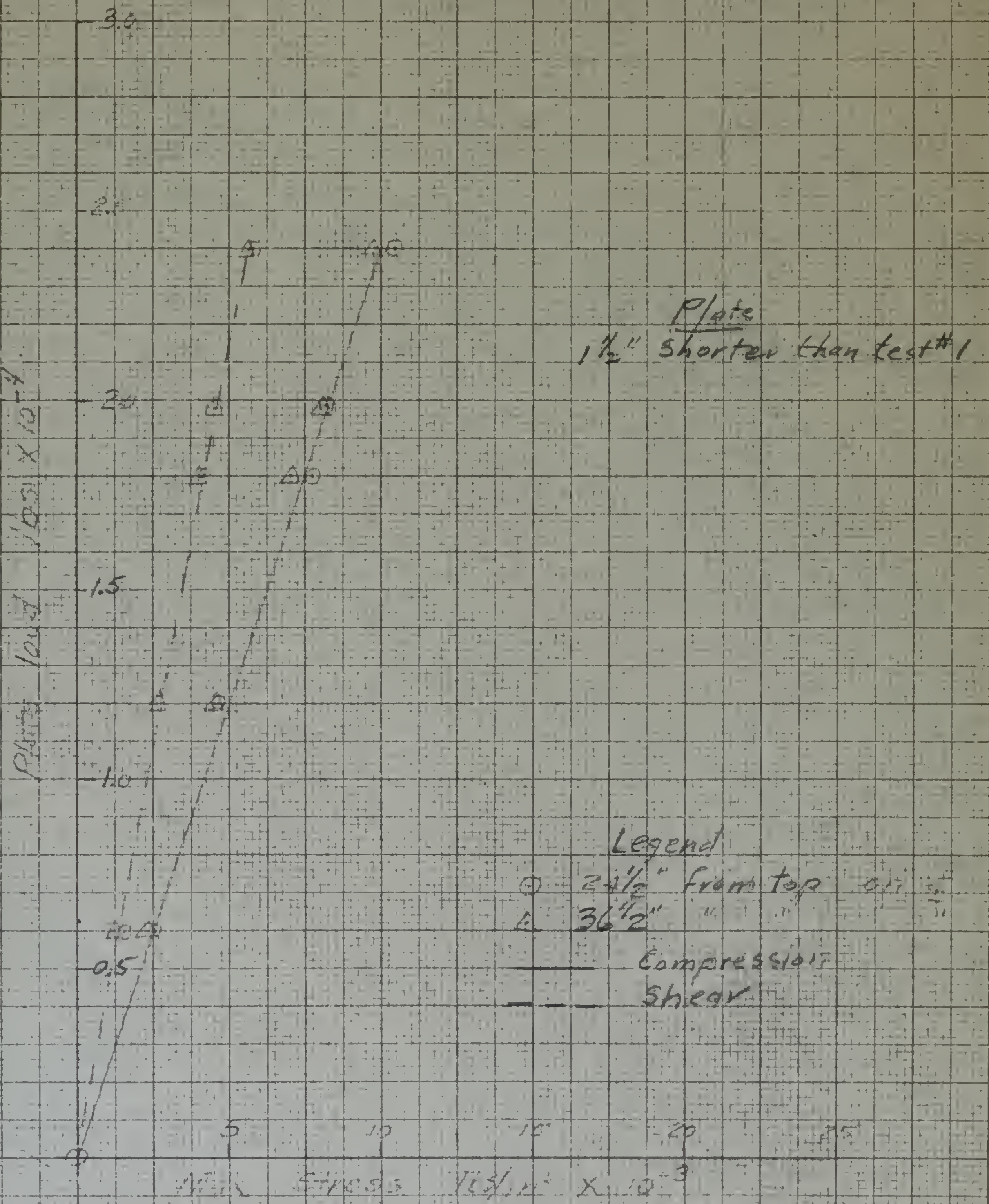

Plate
1½" shorter than test #1

Fig. 10

Plate Load vs. Max Corrugation Stress

(Test #2)

Ref. Table II

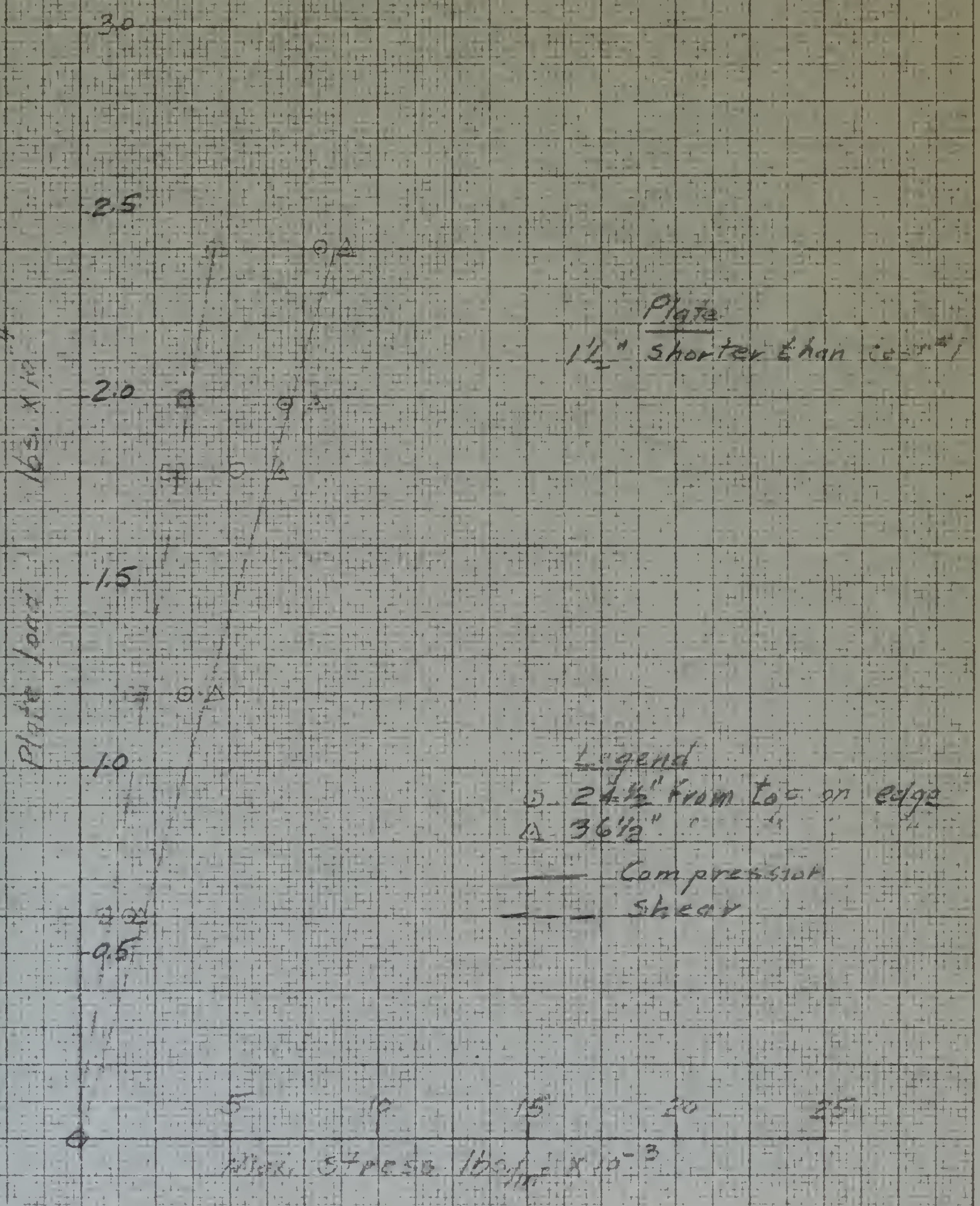

Fig. 11

Plate Load vs. Max. Cover Sheet (1) Stress

(Test #3 Extrusion)

Ref Table IV

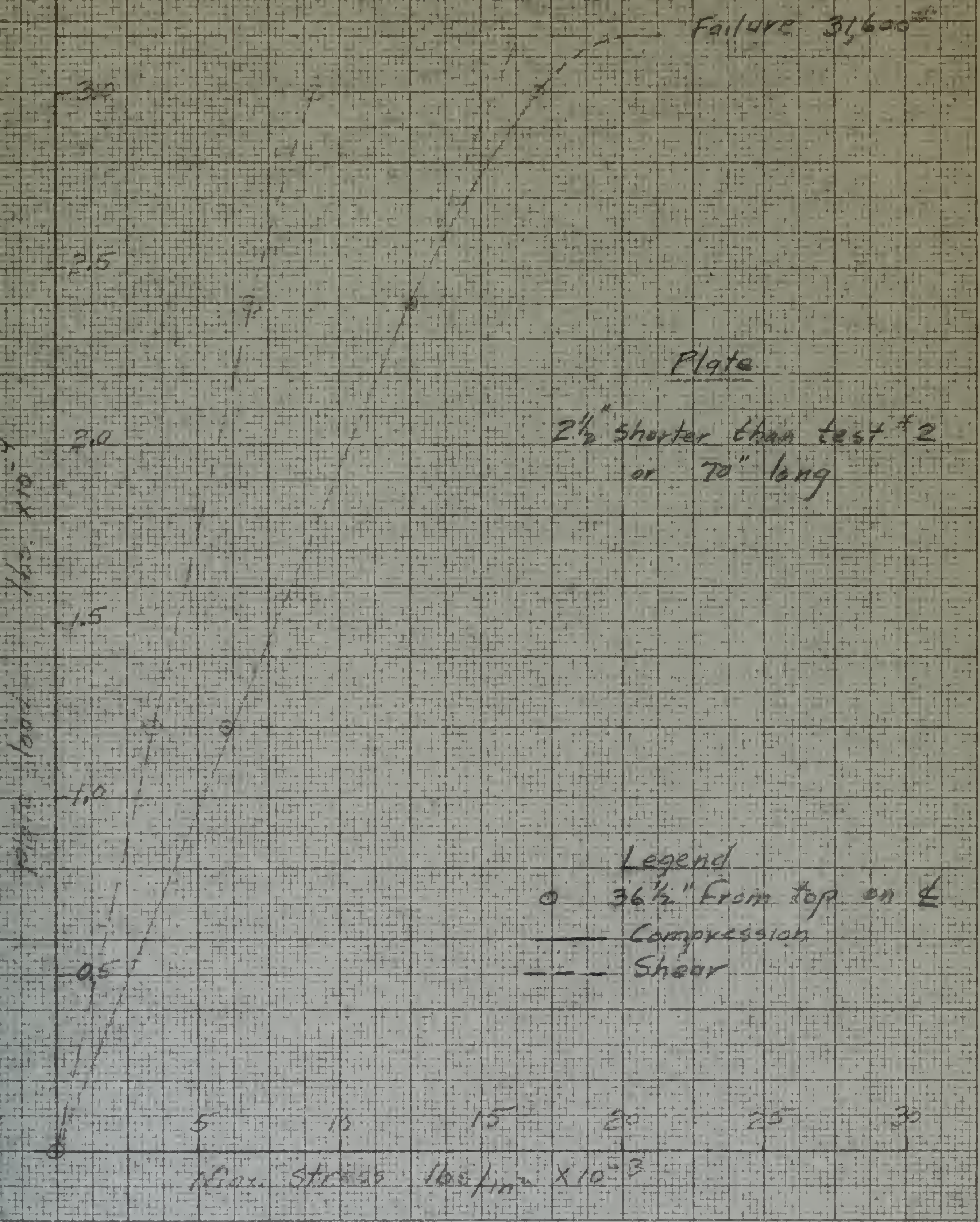

Fig. 12

Plate Load vs Max Cover Sheet(2) Stress
(Test #3 Destruction) Ref. Table III

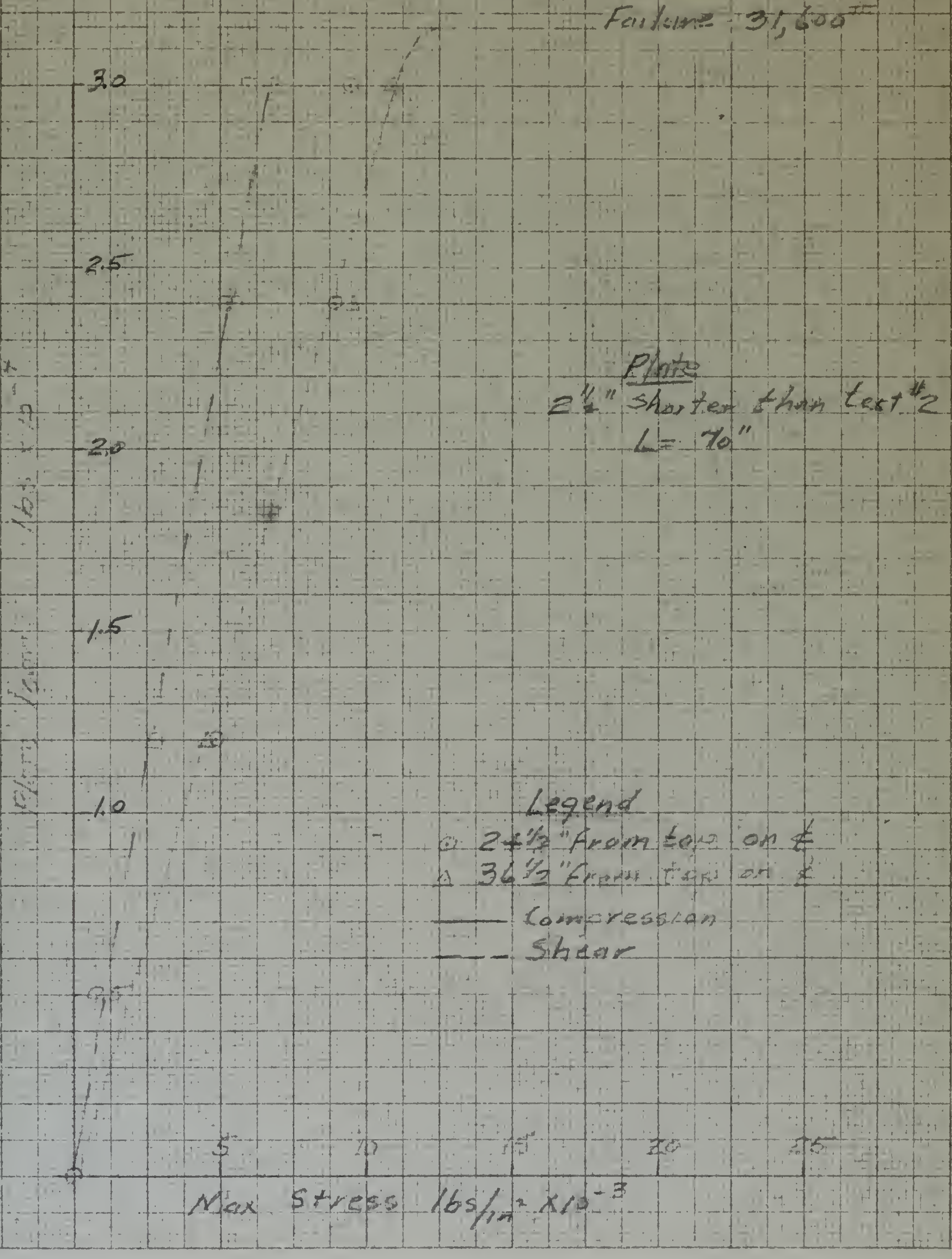

Fig. 13

Plate Load vs. Max Corrugation Stress
(Test #3) Ref Tab III

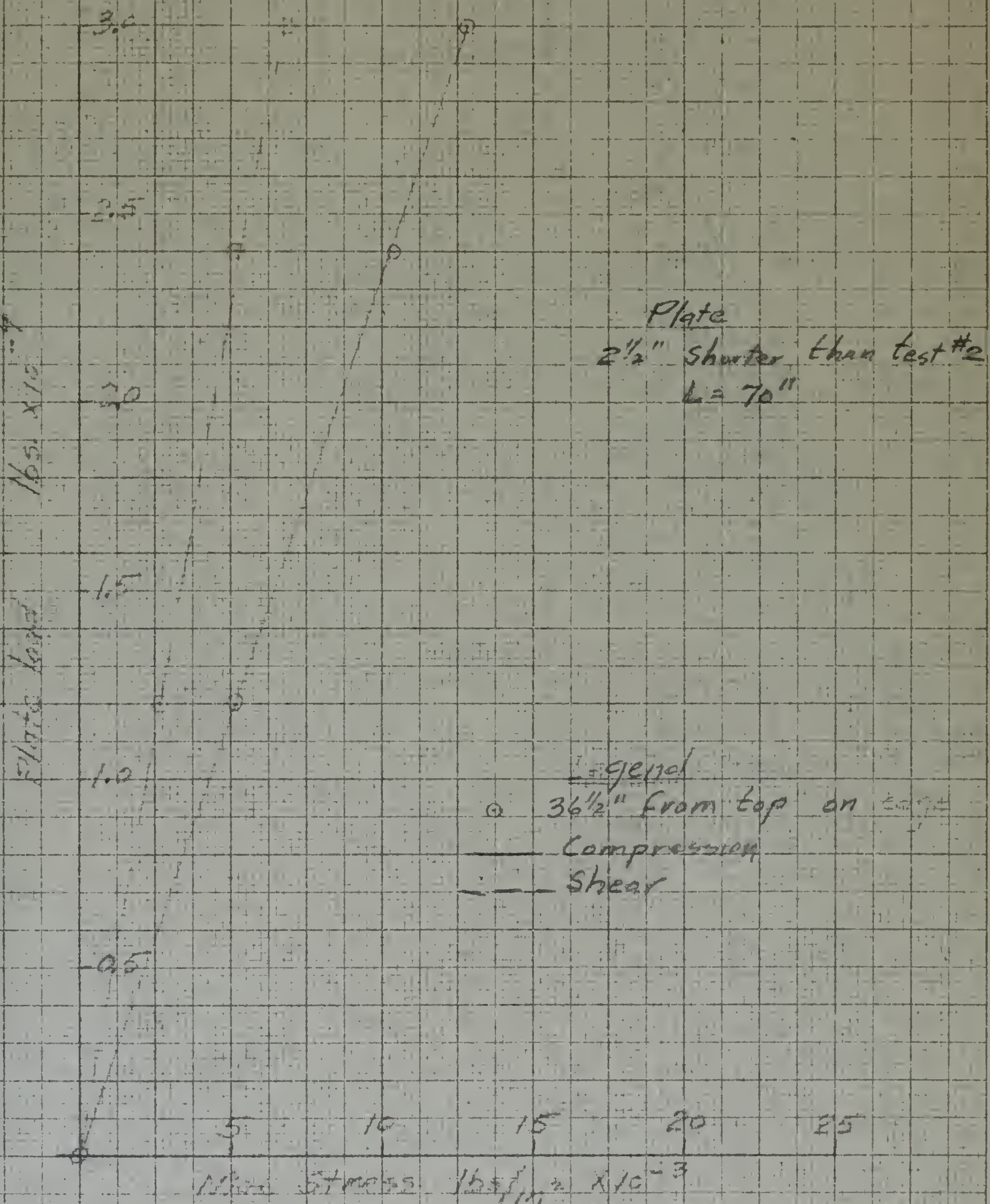

Plate
2½" Shorter than test #2
L = 70"

Fig. 14

Plate Load vs. Maximum Stress
(Test # 4 Destruction)
Ref. Table IV

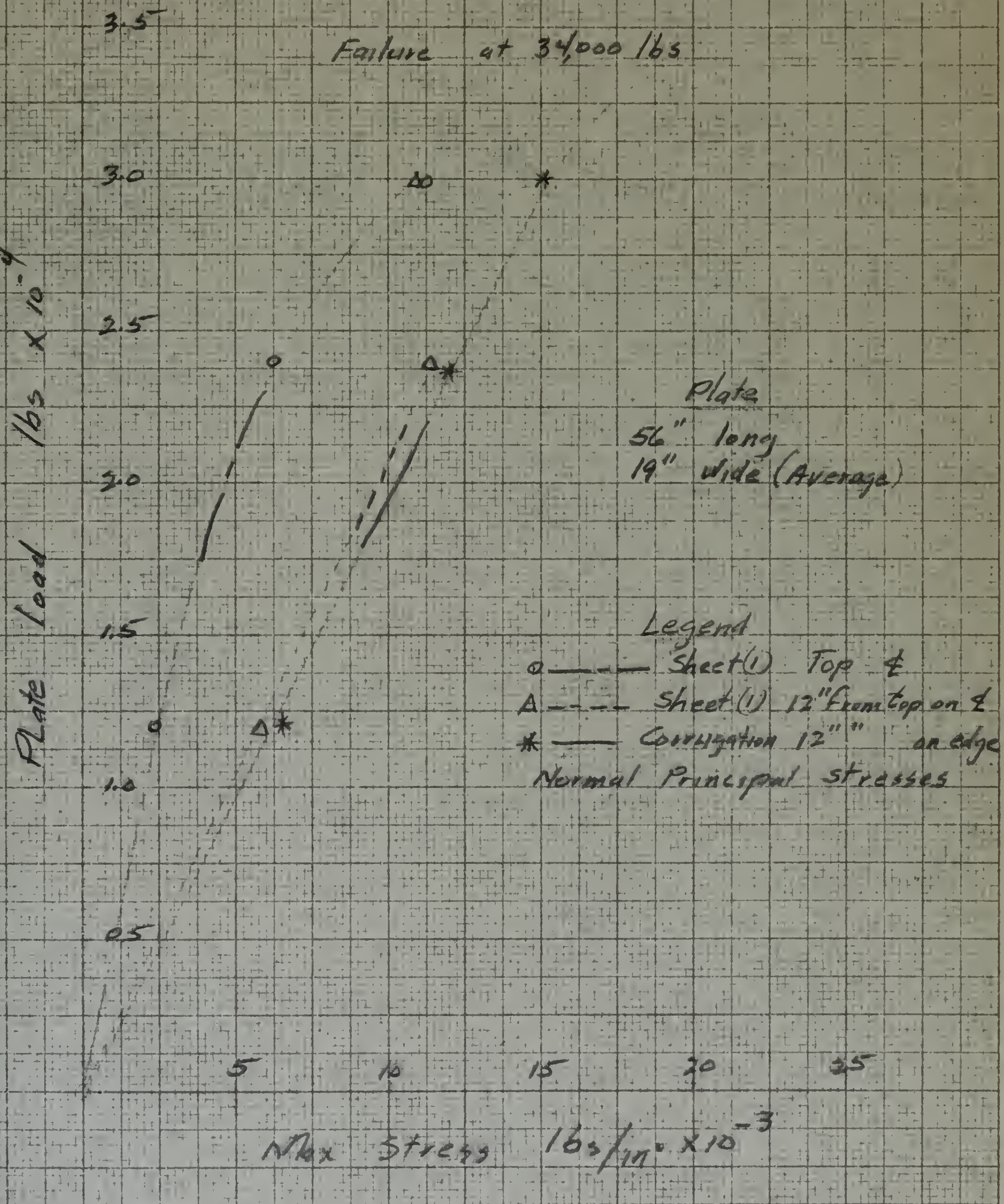

Fig. 15

Sheet and Corrugation
Properties
(Average Section)

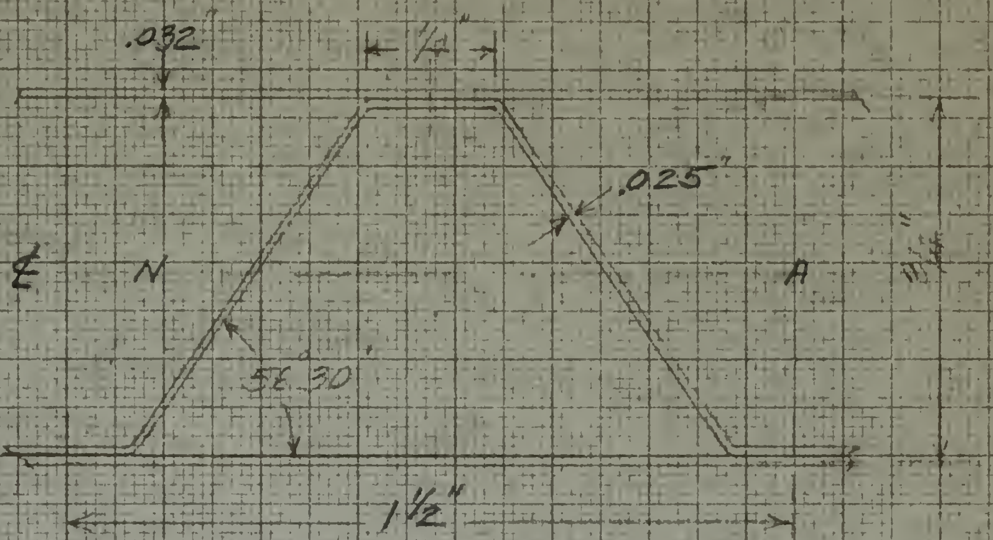

Sheet and Corrugation joint
by 1/8" cherry rivets
on both sides

Properties

Sheet

$A = 0.064\ in^2/in$
$I = 0.00765\ in^4/in$ {bare properties}
14 ST Alclad
$t_s = 0.0272$ bare

Corrugation

$A = 0.0357\ in^2/in$
$I = 0.00245\ in^4/in$ {bare properties}
3cl-T Alclad
$t_c = 0.0222$ bare

Fig. 16
Sheet and Corrugation
Properties
(Minimum Section)

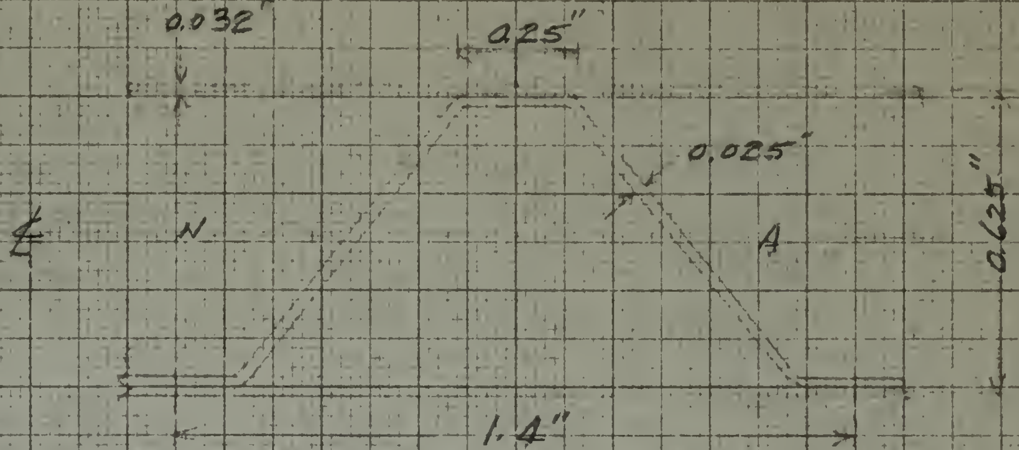

Sheet and Corrugation joined
by 1/8" Cherry rivets
on both Sides

## Properties

Sheet
$A = 0.064$ in$^2$/in
$I = 0.005475$ in$^4$/in {bare properties}
$t_s = 0.0272$ in. bare
14 S-T Alclad

Corrugation
$A = 0.0375$ in$^2$/in
$I = 0.00159$ in$^4$/in
$t_c = 0.0222$ in. bare
301-T Alclad

Fig. 17

Compression Properties 301-T, 14S-T Alclad sheet

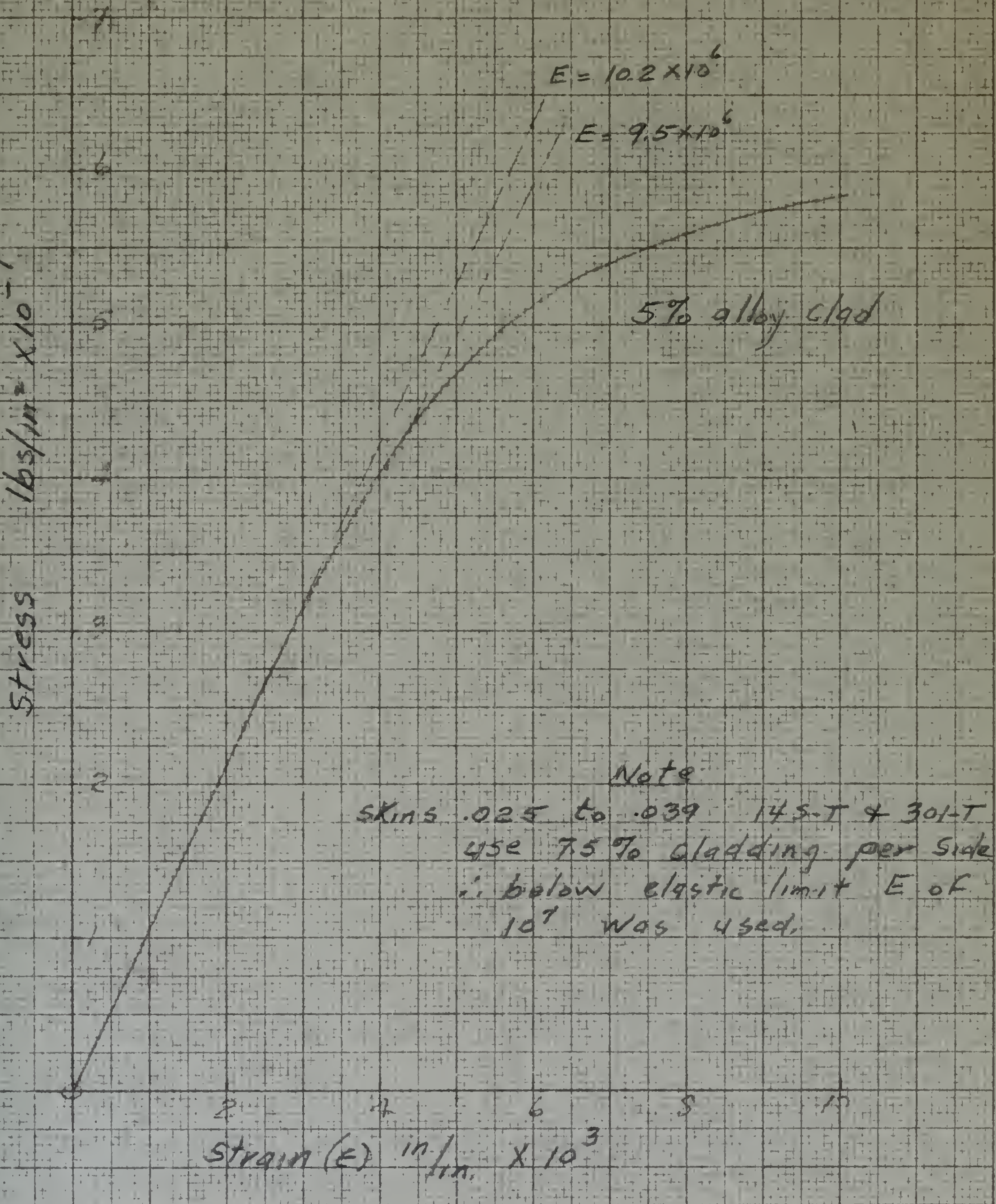

Note

Skins .025 to .039 14S-T + 301-T
use 7.5% cladding per side
∴ below elastic limit E of
$10^7$ was used.

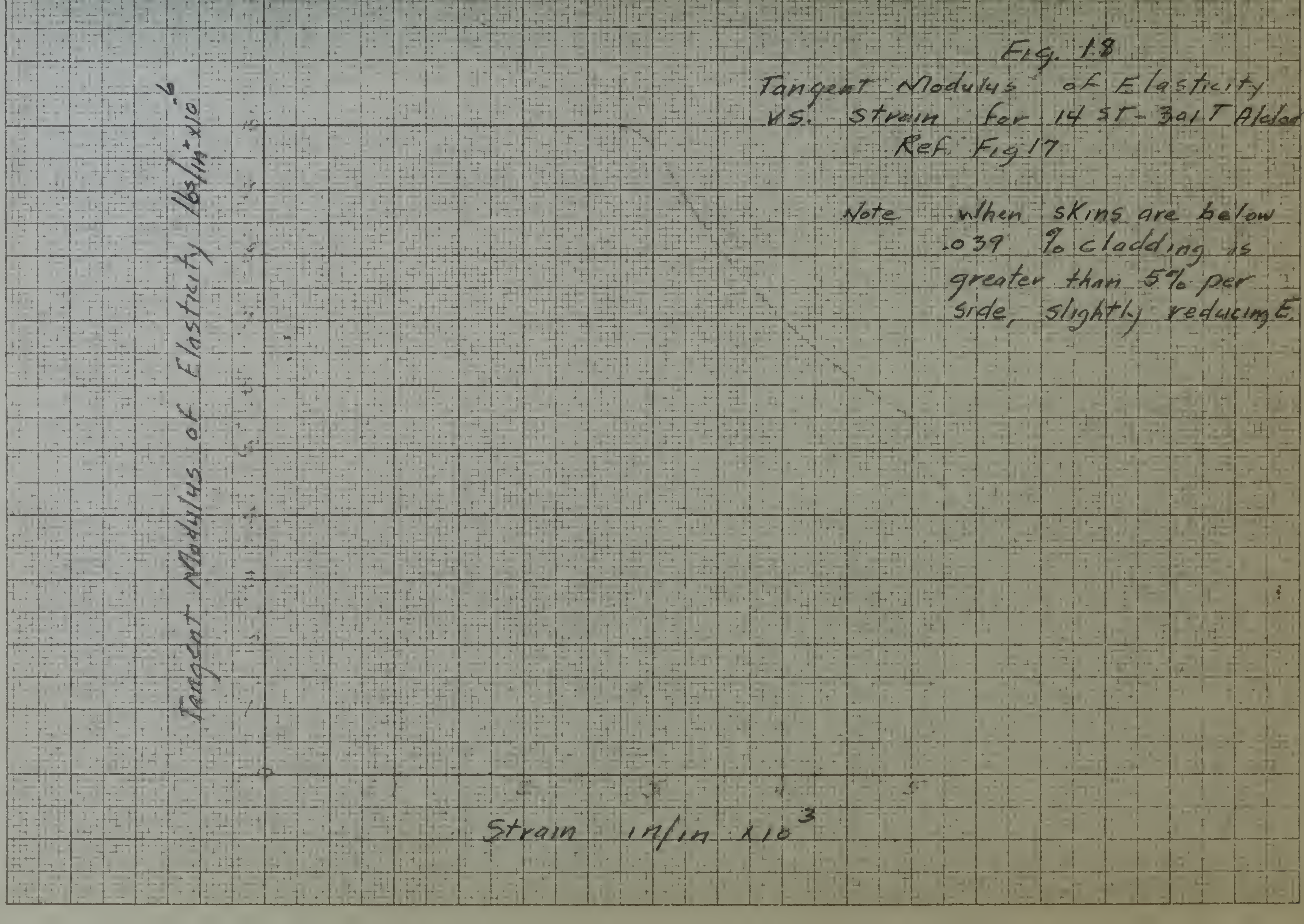

Fig. 18

Tangent Modulus of Elasticity
vs. Strain for 14 ST-3al T Alclad
Ref. Fig 17

Note when skins are below
.039 % cladding is
greater than 5% per
side, slightly reducing E.

Fig. 19
Average Stress of sheet vs. Strain beyond initial instability point of sheet

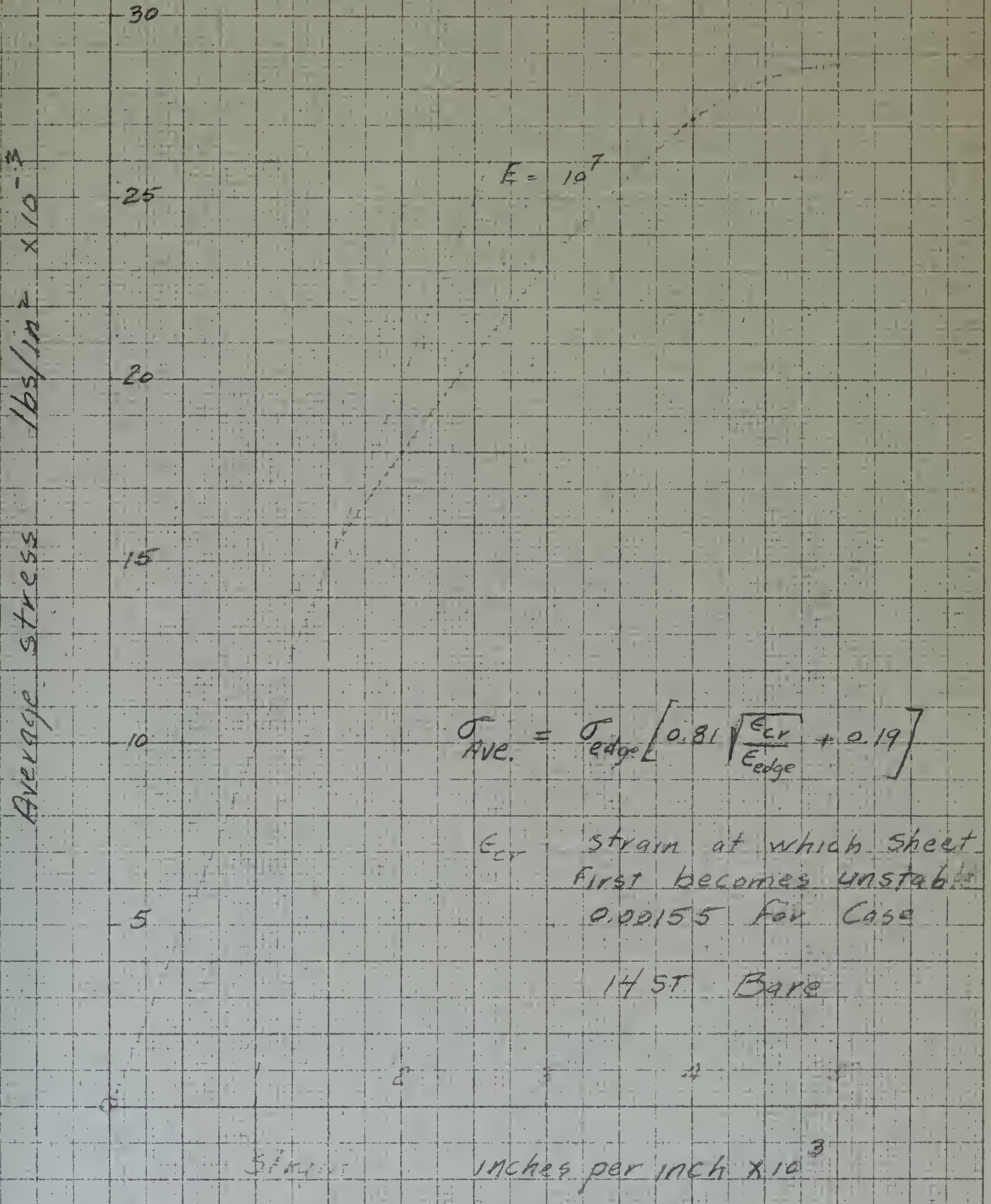

$$\sigma_{Ave.} = \sigma_{edge}\left[0.81\sqrt{\frac{\epsilon_{cr}}{\epsilon_{edge}}} + 0.19\right]$$

$\epsilon_{cr}$ strain at which sheet first becomes unstable 0.00155 for Case

14 ST Bare

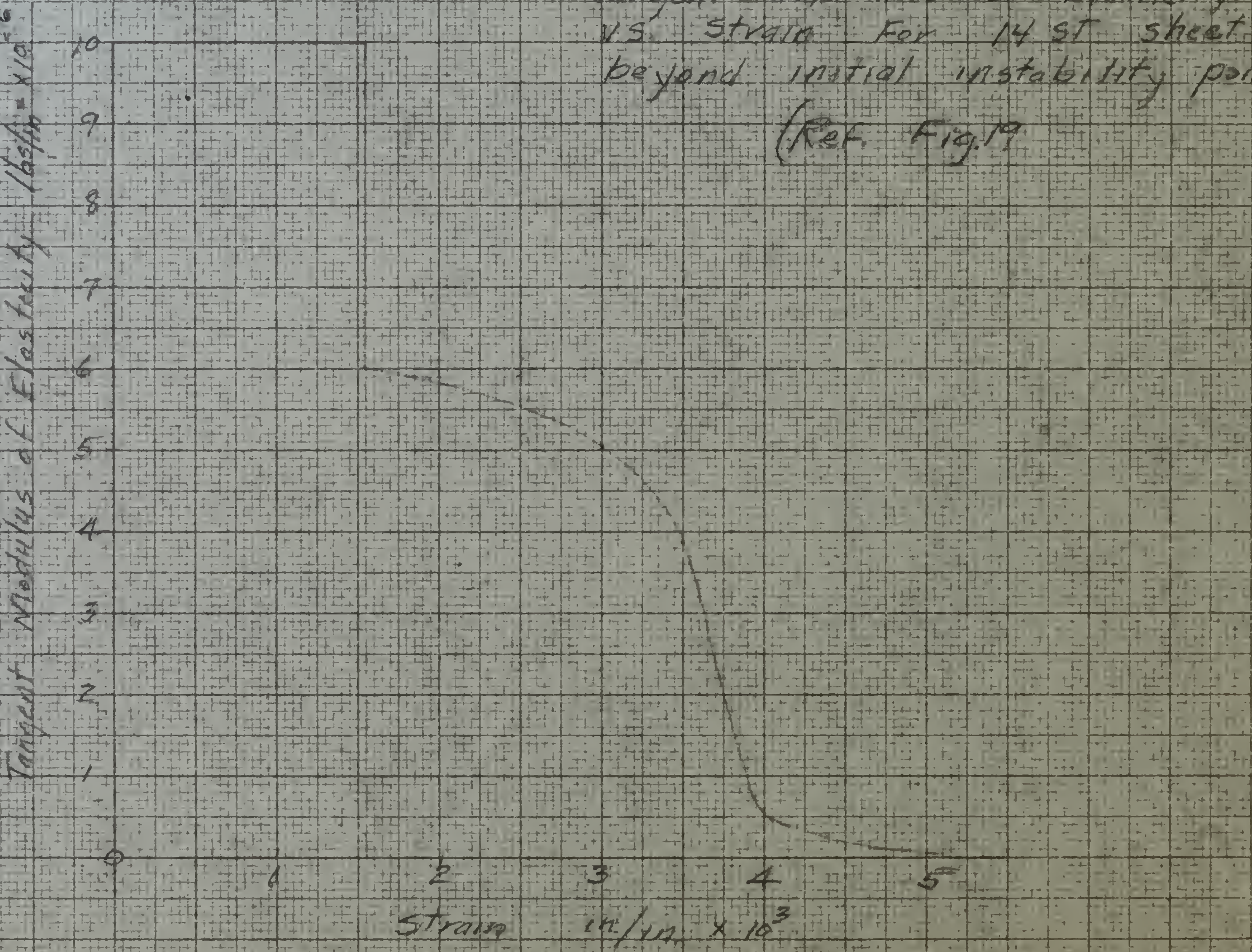

Fig. 20

Tangent Modulus of Elasticity
vs. Strain For 14 ST sheet
beyond initial instability point

(Ref. Fig. 19

Fig. 21

Predicted Critical Plate Load

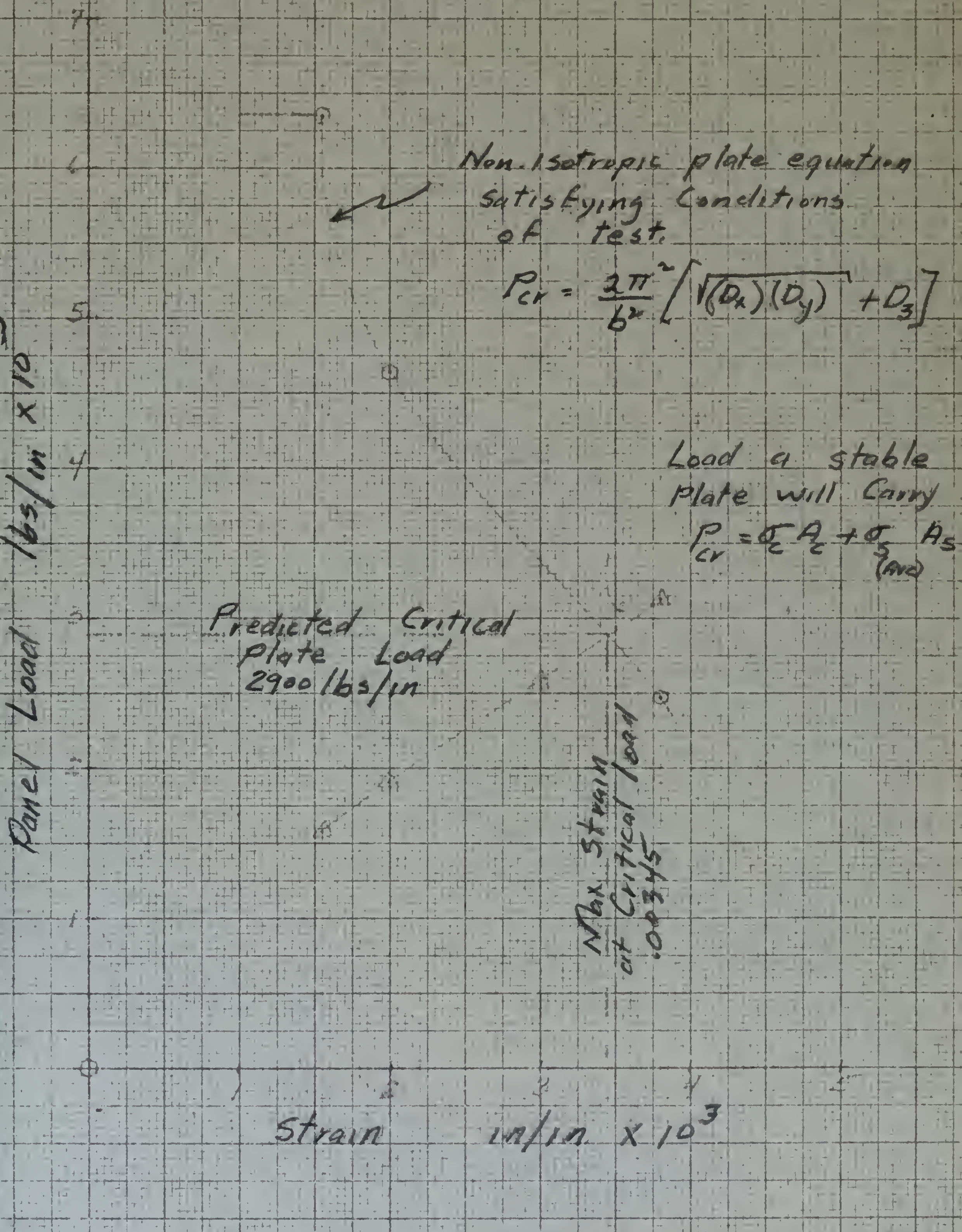

thesl57
Analysis of a double skin and corrugated

3 2768 002 10179 2
DUDLEY KNOX LIBRARY